Published online 28 February 2021

Nucleic Acids Research, 2021, Vol. 49, No. 6 ***3409–3426***
doi: 10.1093/nar/gkab117

RNA thermoswitches modulate *Staphylococcus aureus* adaptation to ambient temperatures

Arancha Catalan-Moreno[1], Marta Cela[1], Pilar Menendez-Gil[1], Naiara Irurzun[1], Carlos J. Caballero[1], Isabelle Caldelari[2] and Alejandro Toledo-Arana[1,*]

[1]Instituto de Agrobiotecnología, IdAB, CSIC-Gobierno de Navarra, Avda. de Pamplona 123, 31192 Mutilva, Navarra, Spain and [2]Architecture et Réactivité de l'ARN, Université de Strasbourg, CNRS, UPR 9002, F-67000 Strasbourg, France

Received October 10, 2020; Revised January 27, 2021; Editorial Decision February 09, 2021; Accepted February 11, 2021

ABSTRACT

Thermoregulation of virulence genes in bacterial pathogens is essential for environment-to-host transition. However, the mechanisms governing cold adaptation when outside the host remain poorly understood. Here, we found that the production of cold shock proteins CspB and CspC from *Staphylococcus aureus* is controlled by two paralogous RNA thermoswitches. Through *in silico* prediction, enzymatic probing and site-directed mutagenesis, we demonstrated that *cspB* and *cspC* 5′UTRs adopt alternative RNA structures that shift from one another upon temperature shifts. The open (O) conformation that facilitates mRNA translation is favoured at ambient temperatures (22°C). Conversely, the alternative locked (L) conformation, where the ribosome binding site (RBS) is sequestered in a double-stranded RNA structure, is folded at host-related temperatures (37°C). These structural rearrangements depend on a long RNA hairpin found in the O conformation that sequesters the anti-RBS sequence. Notably, the remaining *S. aureus* CSP, CspA, may interact with a UUUGUUU motif located in the loop of this long hairpin and favour the folding of the L conformation. This folding represses CspB and CspC production at 37°C. Simultaneous deletion of the *cspB*/*cspC* genes or their RNA thermoswitches significantly decreases *S. aureus* growth rate at ambient temperatures, highlighting the importance of CspB/CspC thermoregulation when *S. aureus* transitions from the host to the environment.

INTRODUCTION

The ability of pathogens to adapt to the ever-changing environmental conditions and survive outside the host under different settings is crucial for their dissemination and transmission. Their persistence on inanimate surfaces increases the risk of new host colonization and outbreaks if no regular preventive measures are taken (1). Most pathogenic bacteria, such as *Enterococcus* spp., *Staphylococcus aureus*, *Escherichia coli* or *Streptococcus pyogenes*, can survive on dry surfaces for months (2–5).

In recent years, environmental contamination by *S. aureus* has been recognized as a potential threat to humans (6). Approximately 20–30% of the human population are *S. aureus* carriers, who are responsible for its spread and colonization of the surface of a wide variety of items. Some of these include bathroom sinks, remote controls, toilet seats, computers, towels and mobile phones. The ability of *S. aureus* to survive for long periods of time in such diverse environments has been linked to reinfections and new host colonizations (7,8). The adaptability and opportunistic nature of this bacterium allow it to cause both hospital- and community-acquired infections, which range from superficial skin abscesses or catheter-associated infections to more serious and life-threatening events such as surgical infections, osteomyelitis, septicemia, endocarditis or pneumonia. Moreover, its capacity to resist almost all available antibiotics makes it one of the most clinically relevant pathogens worldwide (9,10).

One of the main variables that bacteria need to face when leaving the host is the shift in temperature. In general, bacterial physiology is reprogrammed through the activation of adaptive systems in response to new temperatures, which may be sensed through conformational changes of protein, DNA and RNA molecules (11–13). Exposure to low temperatures leads to the induction of members of the cold shock protein (CSP) family, which modulate changes in cell size, wall thickness and metabolic homeostasis (14–16). The cold shock adaptation process has been largely investigated in the Gram-negative bacterial model *E. coli*, which encodes nine CSPs (17–20). When simultaneously lacking four out of these nine variants, *E. coli* shows a growth defect at cold temperatures (19). In

*To whom correspondence should be addressed. Tel: +34 948 16 9752; Email: a.toledo.arana@csic.es

Gram-positive bacteria such as *Listeria monocytogenes*, *csp* genes are significantly induced in cold-adapted cells and bacterial growth is completely abolished in a *cspA* mutant at 4°C (21). A similar phenomenon has also been reported for *Bacillus subtilis*, *Lactococcus lactis* and *S. aureus*, when lacking one or specific combinations of the *csp* genes (22–26).

It is believed that post-transcriptional mechanisms drive the cold shock response in bacteria (27–29). When *E. coli* cells are exposed to cold, protein translation is severely decreased due to mRNA structural reorganizations that prevent optimal ribosome progression; hence, bacterial growth is arrested for about 6 h (20,30). Importantly, in contrast to other proteins, CspA production is drastically increased shortly after the temperature drops. This occurs due to rearrangements in its highly structured 5′UTR that result in a more favourably translated conformation. Once CspA reaches a sufficient concentration inside the cell, it destabilizes RNA structures that would otherwise impair translation at low temperatures (20,28,30,31). The presence of alternative structures in the *E. coli cspA* 5′UTR at 37°C and at cold temperatures (10 and 20°C) has been demonstrated through enzymatic and chemical probing as well as site-specific mutagenesis studies (20,28). This supports the idea of the *cspA* mRNA acting as an RNA thermosensor that adopts a less compact and more actively translated conformation at ambient temperatures, as opposed to the classical RNA thermometers, which generally favour translation at higher host-related temperatures (20,28,32). Interestingly, a recent report showed the presence of a similar RNA thermoswitch in the 5′UTR of the *L. monocytogenes cspA* mRNA that controls the expression of CspA through temperature-dependent alternative RNA structures (33). In addition, the increased translation of other CSPs at low temperatures is known to be modulated via their 5′UTRs; however, the molecular mechanisms responsible for it remain poorly understood (18,20,31,34,35).

The *S. aureus* genome encodes three CSP paralogues (CspA, CspB and CspC) with a protein identity >70% between them (36). It has been shown that the *cspB* mRNA levels are induced after cold shock (25,26), while the *cspA* mRNA levels remain unaltered by shifts in the temperature (37). Nevertheless, as it is the case with most bacteria, there is no knowledge of how CSP expression is coordinated at the protein level and whether they are required for *S. aureus* adaptation to environmental changes. In this study, we demonstrate that the production of two out of the three *S. aureus* CSPs is activated through a drop in temperature. This occurs when the pathogen transitions from host-related (37°C) to ambient temperatures (e.g. 22 and 28°C). The thermoregulation of CspB and CspC occurs at the post-transcriptional level through the action of two paralogous thermosensitive RNA elements located at the 5′UTR of the *cspB* and *cspC* mRNAs, respectively. We also show that the temperature-dependent repression of CspB and CspC requires the action of CspA. In addition, we predict that similar RNA thermoswitches may be involved in the control of CSP expression in several bacterial species.

MATERIALS AND METHODS

Strains, plasmids, oligonucleotides and growth conditions

The bacterial strains, plasmids and oligonucleotides used in this study are listed in Supplementary Tables S1–S3, respectively. *Staphylococcus aureus* strains were grown in Mueller–Hinton (MH) broth (Sigma-Aldrich), whereas *E. coli* was grown in LB broth (Pronadisa). The B2 (casein hydrolysate, 10 g/l; yeast extract, 25 g/l; NaCl, 25 g/l; K_2HPO_4, 1 g/l; glucose, 5 g/l; pH 7.5) and SuperBroth (tryptone, 30 g/l; yeast extract, 20 g/l; MOPS, 10 g/l; pH 7) media were used to prepare *S. aureus* and *E. coli* competent cells, respectively. For selective growth, media were supplemented with the appropriate antibiotics at the following concentrations: erythromycin, 1.5 μg/ml or 10 μg/ml; ampicillin, 100 μg/ml.

RNA structure predictions

To address the alternative conformations of the 5′UTRs, RNA structure predictions were carried out using both the last and the previous 2.3 mfold versions found at http://mfold.rna.albany.edu/?q=mfold/RNA-Folding-Form (38). Different 5′UTR lengths were used as queries and the default parameters were applied. All structures predicted by mfold were inspected and compared. Vienna format files from prediction results of interest were downloaded and used to draw the putative RNA structures using the VARNA software (39). Note that during the revision of this manuscript, the mfold web server was discontinued. If this situation remains unresolved over time, researchers aiming to predict alternative structures in their CSP of interest and/or reproduce our results should use RNAstructure web server (https://rna.urmc.rochester.edu/RNAstructureWeb/Servers/Predict1/Predict1.html) instead. We have obtained similar results with both web servers.

Plasmid constructions

The plasmids used in this study (Supplementary Table S2) were engineered as previously described (40). Briefly, the PCR fragments were amplified from chromosomic or plasmidic DNA with the DreamTaq DNA polymerase (Thermo Scientific) using the appropriate oligonucleotides listed in Supplementary Table S3. The PCR products were purified from agarose gels using the Macherey-Nagel NucleoSpin Gel and PCR Clean-up Kit (Thermo Scientific). The purified products were then ligated into the cloning vector pJET 1.2 (Thermo Scientific) and used to transform the *E. coli* XL1-blue or IM01B cells. DNA fragments were excised using the corresponding FastDigest restriction enzymes (Thermo Scientific) and ligated into the final vector with the Rapid DNA Ligation Kit (Thermo Scientific). All constructs were verified by Sanger sequencing and electroporated into *S. aureus* competent cells (41).

The pMAD plasmids (pMAD_*cspB*^{3xF}, pMAD_*cspC*^{3xF}, pMAD_Δ24*cspB*, pMAD_Δ24*cspC*, pMAD_Δ24*cspB*^{3xF}, pMAD_Δ24*cspC*^{3xF}) were used for chromosomal mutations, either to insert the 3xFLAG tag or to delete the first 24 nucleotides from the *cspB* and *cspC* mRNAs, respectively. Briefly, the flanking regions (AB and CD) from the target

genes were amplified using specific oligos A/B and C/D (Supplementary Table S3). The flanking regions were amplified by an overlapping PCR using primers A and D and ligated into pJET. The resulting vectors were digested and the fragments corresponding to the flanking regions were inserted into a previously excised pMAD vector.

The pHRG plasmid expressed the *gfp* gene under the control of the Phyper promoter (42), whose sequence was adapted from the promoter that drives transcription of early genes in the SP01 *B. subtilis* bacteriophage to include an EcoRI site upstream of the native transcriptional start site (43). This plasmid was constructed by PCR amplification using the pCN57 plasmid (44) as a template and oligonucleotides phyper-RBSicaR-GFP and GFPend-AscI (Supplementary Table S3). The amplified product was ligated into pJET. The resulting vector was digested using SphI and AscI and the fragments of interest were inserted into the pCN47 plasmid (44). Plasmids p5′UTR^{cspB}-*gfp* and p5′UTR^{cspC}-*gfp* were generated by amplifying the 5′UTR sequences from the pCspB^{3xF} and pCspC^{3xF} plasmids (36) with oligonucleotide pairs 5UTR_CspB_FW_EcoRI/5UTR_CspB_RV_SpeI and 5′UTR_CspC_FW_EcoRI/5′UTR_CspC_RV_SpeI (Supplementary Table S3), respectively. The amplified PCR products were then digested using the EcoRI and SpeI enzymes and ligated into pHRG. Similarly, the plasmids for mutating 5′UTRs were constructed by PCR amplification from p5′UTR^{cspB}-*gfp* or p5′UTR^{cspC}-*gfp* using the corresponding 5′UTR mutated forward oligonucleotides (Supplementary Table S3) and 5UTR_CspB_RV_SpeI or 5′UTR_CspC_RV_SpeI (Supplementary Table S3). The amplified fragments were then digested with EcoRI/SpeI and ligated into the pHRG plasmid. The resulting vectors were named p5′UTR^{cspB}Δ24-*gfp*, p5′UTR^{cspC}Δ24-*gfp*, p5′UTR^{cspB}UAU47AA-*gfp*, p5′UTR^{cspB}C50G-*gfp*, p5′UTR^{cspB}UU55AA-*gfp*, p5′UTR^{cspB}UU55AA+UU26AA-*gfp*, p5′UTR^{cspC}UU48A-*gfp* and p5′UTR^{cspB}U38C+U41C-*gfp* (Supplementary Table S2).

Generation of *csp* mutants by homologous recombination

The *csp* mutant strains were obtained by marker-less homologous recombination, using the pMAD plasmid system (45) as previously described (36). Briefly, the *cspB*^{3xF}, *cspC*^{3xF}, *cspB*^{3xF}Δ*cspA*, *cspC*^{3xF}Δ*cspA*, Δ*cspBC*, Δ*24cspB*, Δ*24cspC*, Δ*24cspB*^{3xF}, Δ*24cspC*^{3xF} and Δ*24cspBC* strains were generated by a two-step procedure that inserts or replaces a gene of interest by a mutant allele contained within the pMAD plasmids (Supplementary Table S2) (46). The resulting mutant strains were confirmed by PCR using the corresponding oligonucleotides E and F (Supplementary Table S3). In addition, the PCR fragments were verified by Sanger sequencing.

Bacterial cultures for total protein extraction and western blotting

Staphylococcus aureus cultures were grown in Erlenmeyer flasks containing MH broth supplemented with 10 μg/ml erythromycin. Media were inoculated (1:250) with normalized bacterial aliquots, which were previously grown at 37°C and 200 rpm overnight. Bacterial cultures were incubated at different temperatures (22, 28 and 37°C) and 200 rpm until cells reached an early exponential phase (OD_{600nm} = 0.4). Cultures were harvested by centrifugation for 10 min at 4400 × *g* and 4°C. Bacterial pellets were stored at −80°C until required. Pellets were thawed and washed with 700 μl of 1× phosphate-buffered saline (PBS). Next, bacteria were placed in Lysing Matrix B tubes containing acid-washed 100 μm glass beads (Sigma) and lysed for 45 s and speed 6 using a FastPrep-24 instrument (MP Biomedicals). This step was repeated once and the tubes were centrifuged for 10 min at 21 000 × *g* and 4°C. The supernatants containing the total protein extracts were transferred to Eppendorf tubes. Total proteins were quantified using a Bradford protein assay (Bio-Rad) and samples were prepared at the desired concentration in Laemmli buffer. Samples were stored at −20°C until needed.

Western blot analyses were performed as previously described (36). The chromosomally 3xFLAG-tagged CSPs were developed with anti-FLAG antibodies (Sigma) and the GFP samples with monoclonal anti-GFP antibodies 1:5000 (Living Colors, Clontech) and peroxidase-conjugated goat anti-mouse immunoglobulin G and M antibodies 1:2500 (Pierce-Thermo Scientific). Membranes were developed in a ChemiDoc Imaging System using the SuperSignal West Pico Chemiluminescent Substrate Kit (Thermo Scientific). Protein levels of three independent replicates were quantified by measuring band intensity with ImageJ (https://imagej.nih.gov/ij/).

RNA extraction and northern blotting

Bacteria were cultured as mentioned in the previous section. Cultures were centrifuged for 3 min at 4400 × *g* and 4°C. Pellets were then frozen in liquid nitrogen and stored at −80°C until needed. RNA extractions were performed as previously described (47). An appropriate amount of RNA was mixed with formaldehyde loading dye (Ambion), denatured for 15 min at 65°C and run in 1.25% agarose gels with Midori Green (Teknovas). Gels were checked for RNA integrity and appropriate loading under UV light exposure. RNAs were then transferred to 0.2 μm pore size Nitran N membranes (GE Healthcare Life Sciences) by capillarity using the NorthernMax Transfer Buffer (Ambion), for 1.5 h at room temperature. The transferred RNAs were cross-linked to the membranes by exposing them to UV light with a UV Stralinker 1800 (Stratagene). Membranes were then prehybridized using ULTRAHyb solution (Ambion) for at least 30 min at 40°C in a rotating oven. After the prehybridization step, the corresponding oligonucleotide probes (anti_3xFLAG_probe or anti-GFP probe) (Supplementary Table S3) were radioactively labelled with [γ-^{32}P]-ATP (Perkin Elmer) following the manufacturer's recommendation. Probes were then purified with Illustra MicroSpin G-50 columns (GE Healthcare) and incubated with membranes at 40°C overnight. Membranes were washed three times for 5 min with preheated 2× SCC, 0.1% SDS at 40°C followed by at least two washing steps of 0.1× SCC, 0.1% SDS at room temperature until the background signal was non-detectable. Membranes were developed by autoradiography for different time periods. The mRNA levels

from three independent replicates were measured by densitometry of northern blot autoradiographies using ImageJ (https://imagej.nih.gov/ij/).

Molecular beacon assay

The molecular beacon (MB) assay was performed as previously described (48) with the following modifications. Briefly, the *cspB and cspC* ssDNA oligonucleotides (Supplementary Table S3) labelled with the 6-FAM and quencher Iowa Black FQ (IBkFQ) molecules at the 5′ and 3′ ends, respectively, were purchased from Integrated DNA Technologies. The *cspA* ssDNA oligonucleotide (40) was used as a control. Two picomoles of ssDNA oligonucleotides were mixed with 2.5 μl of 10× reaction buffer (100 mM Tris–HCl, pH 7.5, 300 mM KCl, 200 mM NH_4Cl, 15 mM DTT, 50 mM $MgCl_2$) and Milli-Q water up to a final volume of 25 μl. The FAM fluorescence was then measured using the Bio-Rad CFX96 Touch Real-Time PCR Detection System and the following incubation periods: 13°C, 10 min; 18 cycles of 5 min each starting at 16°C and with a 3°C increase per cycle; 5 min at 65°C; and 18 cycles of 5 min each with a 3°C decrease per cycle. FAM emission was registered throughout the incubation steps. Three independent replicates were performed.

In vitro transcription

PCR fragments containing the T7 promoter were amplified using the oligonucleotides listed in Supplementary Table S3. *In vitro* transcription was performed at 37°C using the Megascript T7 transcription kit (Ambion) following the manufacturer's recommendation. RNAs were loaded into a 6% polyacrylamide gel and visualized with UV light after Midori Green (Teknovas) staining. Bands of the appropriate size were cut and the RNA was extracted using 0.5 M ammonium acetate (pH 5.5) at 15°C for 2 h. Next, 1 volume of acid phenol (pH 4.5) was added and samples were incubated at 15°C overnight. After centrifugation for 5 min at 21 000 × *g* and 4°C, RNAs were purified using phenol–chloroform and precipitated by adding 3 volumes of 96% ethanol and 1/10 volume of 3 M sodium acetate (pH 5.5). The mixture was incubated at −80°C for at least 1 h. Samples were then centrifuged for 30 min at 21 000 × *g* and 4°C. Pellets were washed with 70% ethanol, air dried and resuspended in DEPC water (Ambion). The RNA integrity was checked through agarose gel visualization and quantified by the Nanodrop system (Agilent Technologies).

5′-end labelling of RNA

Before labelling, RNAs were dephosphorylated using the FastAP enzyme (Thermo Scientific) at 37°C for 15 min. Inactivation of the enzyme was performed by heat shock at 75°C for 5 min followed by ethanol precipitation supplemented with 1 μl of GlycoBlue™ (Thermo Scientific) coprecipitant. Pellets were resuspended in 20 μl of DEPC water. Dephosphorylated nucleic acids were incubated with [γ-^{32}P]-ATP (Perkin Elmer) and 0.4 U of PNK (Thermo Scientific) for 1 h. Labelled RNAs for enzymatic probing were purified by electrophoresis on a 6% polyacrylamide denaturing gel (8 M urea). The bands of interest were cut from the gel and the RNAs eluted with 400 μl of elution buffer (500 mM $AcNH_4$, 1 mM EDTA and 0.1% SDS) at 4°C overnight. RNAs were then precipitated as previously described and resuspended in 80 μl DEPC water.

Enzymatic probing

The enzymatic probing experiments with RNase T1 and S1 (Thermo Scientific) were performed to determine the *in vitro cspB* and *cspC* 5′UTR structures. Labelled RNAs were first denatured (1 min at 90°C followed by 1 min in ice) and then renatured at 22 or 37°C for 15 min. Two picomoles of labelled RNA was incubated in T1 (RNA structure buffer) or S1 buffer (Thermo Scientific) supplemented with 20 μg yeast tRNA in the presence of different enzyme dilutions (T1: 1×10^{-3}, 2×10^{-2} and 5×10^{-2} U/μl; S1: 5×10^{-5}, 2×10^{-5} and 1×10^{-5} U/μl) for 5 min at 22 or 37°C. In parallel, alkaline hydrolysis and T1 controls were performed to assign the gel bands. Alkaline hydrolysis was accomplished by mixing 2 pmol of labelled RNA with 20 μg of yeast tRNA and 1× alkaline hydrolysis buffer (Thermo Scientific). The mix was then incubated at 95°C for 10 min. For the denaturing T1 reaction, 2 pmol of labelled RNA was preheated with 20 μg yeast tRNA and 1× RNA structure buffer for 3 min at 65°C. Samples were then incubated with 2.5×10^{-2} U/μl of RNase T1 for 1 min 10 s. All reactions were stopped by addition of 40 μl of the Stop Mix solution (0.6 M NaOAc, 4 mM EDTA, 0.1 mg/ml yeast tRNA and 1 μg GlycoBlue) and precipitated with ethanol. The pellets were washed twice with 70% ethanol, air dried and resuspended in 12 μl of loading buffer II (Thermo Scientific). Samples were loaded into a 12% polyacrylamide denaturing gel.

Bacterial growth in TSA plates

For the phenotypic growth experiments in trypticase soy agar (TSA) plates, bacteria were grown in 5 ml of MH broth at 37°C and 200 rpm overnight. The bacterial preinocula were then normalized to an OD_{600nm} of 1. Serial dilutions were plated on TSA plates and incubated at 37°C for 24 h or at 22°C for 72 h.

Survival experiment in synthetic nasal medium

The synthetic nasal medium (SNM3) was prepared as previously described (49) and used for survival experiments of different *S. aureus* strains. Bacteria were grown in 5 ml of MH broth at 37°C and 200 rpm overnight. One millilitre of the preinoculum was centrifuged, washed with 1× PBS and resuspended in 1 ml of SNM3. Bacteria were then diluted 1:250 in 10 ml of SNM3 and grown at 32°C and 200 rpm for 2 days. Next, bacteria were inoculated in fresh SNM3 and grown at 22°C in static conditions in a refrigerated Infors HT Ecotron incubator. Samples were taken at different time points and serial dilutions were plated in TSA. Colony forming units (CFUs) were counted from three independent biological replicates.

Statistical analyses

Statistical significance was determined with the Mann–Whitney *U* test by using GraphPad Prism software. Results

were considered significant if the *P*-value was <0.05, which was indicated as an asterisk in the corresponding plots.

RESULTS

Ambient temperatures induce the production of *S. aureus* CspB and CspC

In order to monitor the expression patterns of CSPs when *S. aureus* grows at different temperatures, we chromosomally tagged the *csp* genes by fusing a 3xFLAG epitope to the C-terminal end. We then incubated the tagged strains in MH medium at 37°C, which is the host-related temperature, and at 22 and 28°C, two different ambient temperatures that *S. aureus* may face when outside the host. Once the bacterial cultures reached the exponential phase ($OD_{600nm} = 0.4$), we extracted their total RNAs and proteins to perform northern and western blot experiments. The results showed that the mRNA expression levels of all three *csp* genes were not significantly affected by changes in the growth temperature (Figure 1A). In agreement with this, when performing western blots, we observed that $CspA^{3xF}$ levels remained invariable, regardless of the growth temperature (Figure 1B). In contrast, $CspB^{3xF}$ and $CspC^{3xF}$ levels were significantly reduced at 37°C when compared to those produced at 22 and 28°C. Note that the highest $CspB^{3xF}$ and $CspC^{3xF}$ protein yields were found at 22°C (Figure 1B). The lack of correlation between the mRNA and protein levels of *S. aureus* CspB and CspC when grown at different temperatures, indicated the presence of putative post-transcriptional regulatory mechanisms controlling the production of both proteins.

Thermoregulation of CspB and CspC is conducted through their 5′UTRs

The existence of post-transcriptional mechanisms that control *S. aureus* CSPs was supported by previous results from our group that showed that CSPs are differentially produced when expressed from the same heterologous promoter (36). Interestingly, our previous transcriptomic maps showed that the *cspB* and *cspC* mRNAs carried long 5′UTRs of 112 and 113 nucleotides, respectively (36,50). Since the 5′UTRs of CSPs in other bacterial models have been reported to undergo thermoregulation (20,23,24,28,33), we tested whether this was the case for the *cspB* and *cspC* 5′UTRs in *S. aureus*. Therefore, we fused both 5′UTRs plus the first five codons of the *cspB* and *cspC* mRNAs to the ATG-less *gfp* gene of the pHRG plasmid, generating the translational reporter plasmids $p5'UTR^{cspB}$-*gfp* and $p5'UTR^{cspC}$-*gfp*, respectively. Note that both reporter gene fusions were under the control of the constitutive promoter Phyper (42), whose sequence was adapted to include an EcoRI site upstream of the native transcriptional start site. We used these plasmids to transform the *S. aureus* wild-type (WT) strain and monitored both the chimeric mRNA levels and GFP protein production. Northen blots results shown in Figure 2A indicated that the chimeric $5'UTR^{cspB}$-*gfp* and $5'UTR^{cspC}$-*gfp* mRNA levels did not significantly change, regardless of the tested temperature (Figure 2A). In contrast, western blots evidenced higher GFP levels at 22 and 28°C when compared to 37°C (Figure 2B).

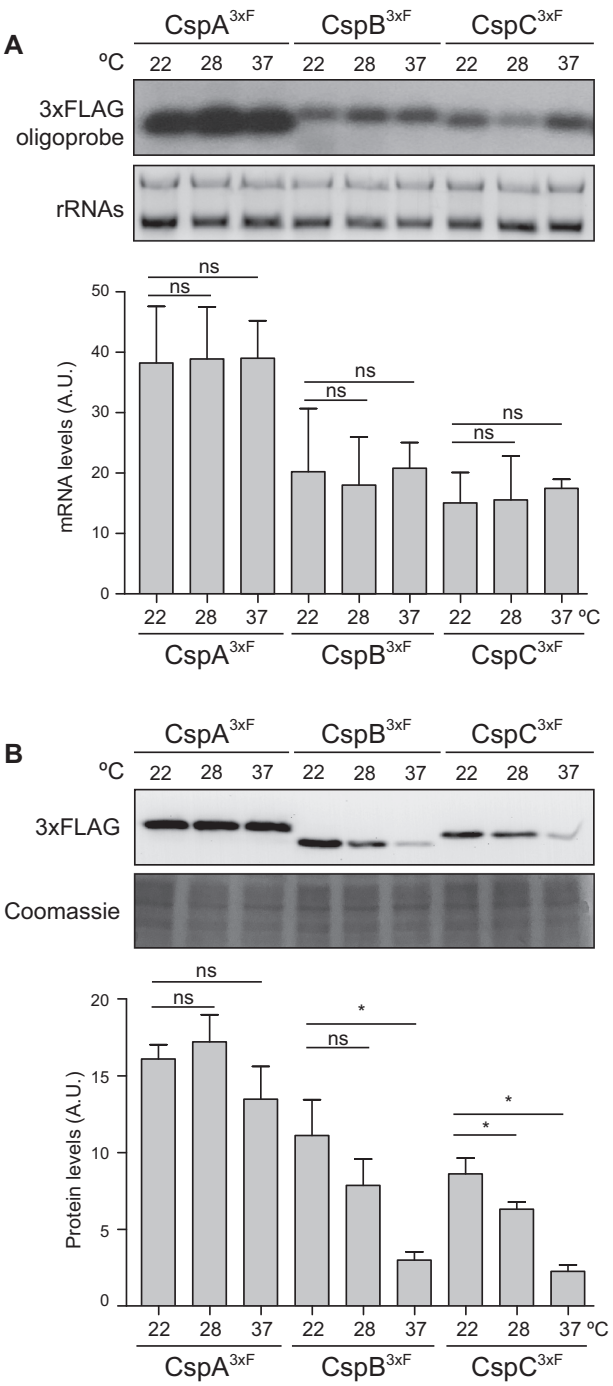

Figure 1. The CspB and CspC protein levels are differentially regulated in response to environmental temperatures. (**A**) Northern blot showing the *csp* mRNA levels, which were detected using a radiolabelled antisense 3xFLAG oligonucleotide probe. Midori Green-stained ribosomal RNAs are included as loading controls. (**B**) Western blot showing the levels of chromosomally 3xFLAG-tagged CSPs, which were developed using peroxidase-conjugated anti-FLAG antibodies and a bioluminescence kit. A Coomassie stained protein gel portion is included as a loading control. Strains were grown until exponential phase ($OD_{600nm} = 0.4$) in MH broth at environmental (22 and 28°C) and host-related (37°C) temperatures. Bar plots represent the mean and standard deviation of the mRNA and protein levels from three independent biological replicates, which were determined by densitometry of mRNA and protein bands using ImageJ (https://imagej.nih.gov/ij/). Asterisks represent statistical significance ($P < 0.05$, Mann–Whitney *U* test); ns, not significant. Representative images from the triplicates are shown.

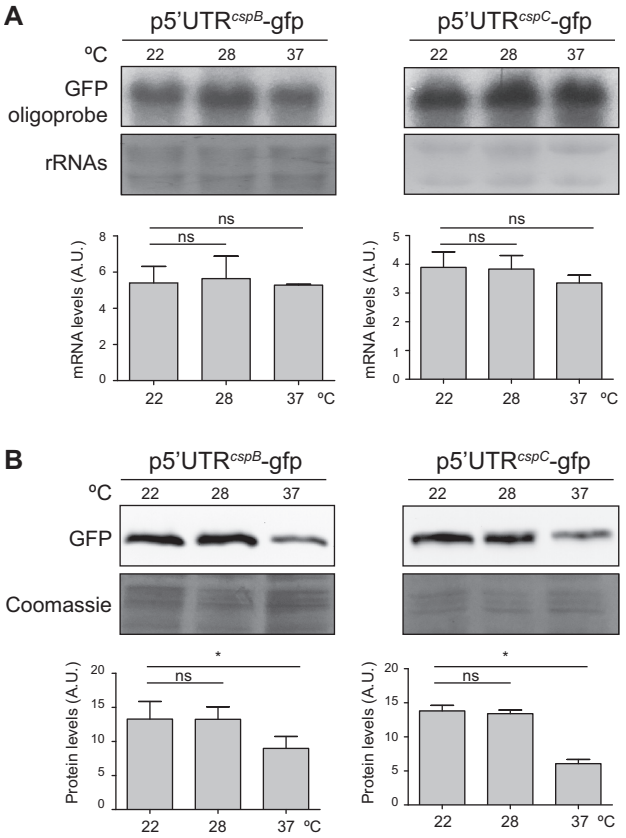

Figure 2. Thermoregulation of the CspB and CspC production is restricted to the *cspB* and *cspC* 5′UTRs, respectively. (**A**) Northern blots showing the 5′UTR-*gfp* chimeric mRNA levels expressed from the corresponding translational reporter strains. Bacteria were grown in MH broth supplemented with the appropriate antibiotic and incubated at 22, 28 and 37°C until exponential phase was reached. Midori Green-stained ribosomal RNAs are included as loading controls. (**B**) Western blots showing the GFP protein levels from the strains expressing the *cspB* and *cspC* 5′UTR-GFP reporter fusions. Membranes were developed using monoclonal anti-GFP, peroxidase-conjugated goat anti-mouse antibodies and a bioluminescent kit. Coomassie stain gel portions are included as loading controls. Bar plots represent the mean and standard deviation of mRNA and protein levels from three independent biological replicates, which were determined by densitometry of mRNA and protein bands using ImageJ (https://imagej.nih.gov/ij/). Asterisks represent statistical significance ($P < 0.05$, Mann–Whitney U test); ns, not significant. Representative images from the triplicates are shown.

These results confirmed that translation of both CspB and CspC proteins was affected by the environmental temperature and that their thermoregulation was dependent on their 5′UTRs.

The *cspB* and *cspC* 5′UTRs adopt mutually exclusive alternative RNA structures

Recently, it was shown that the *cspA* 5′UTRs of *E. coli* and *L. monocytogenes* contain thermoresponsive secondary structure elements, which act as thermosensors that promote CspA expression at low temperatures (20,33). Using the mfold web server (38), we predicted that the *cspB* and *cspC* 5′UTRs (the first 130 nucleotides) in *S. aureus* can fold into two major alternative conformations. Despite minor differences, the *cspB* and *cspC* 5′UTRs displayed extremely similar alternative conformations (Figure 3). One of such conformations included a long and imperfect hairpin that comprised nucleotides ∼3–76 while leaving the ribosome binding site (RBS) exposed. We defined this folding as the 'open' (O) conformation. In contrast, the alternative predicted configuration formed a double-stranded structure through base pairing of nucleotides ∼25–54 with nucleotides ∼100–129 (nucleotide stretch that includes the RBS region). This nucleotide interaction prevented the utilization of the RBS by the translation machinery. For this reason, we named this secondary structure 'locked' (L) conformation (Figure 3). Both alternative conformations were orthologous to the one recently described for the *cspA* 5′UTR of *L. monocytogenes*, despite the lack of sequence similarity between both species (33).

Considering that the 5′UTRs of *cspB* and *cspC* seemed affected by temperature (Figure 2B), we reasoned that such effect might be explained by shifts between the two alternative conformations (O and L) upon temperature changes, as previously described (20,33). Hypothetically, the O conformation would be favoured at lower temperatures, promoting CspB and CspC translation, while the L conformation would be more dominant during *S. aureus* growth at 37°C. To validate this idea, we performed *in vitro* enzymatic structural probing of the *cspB* and *cspC* 5′UTRs at 22 and 37°C using RNases T1 and S1, which cleave unpaired G and A > U > C, respectively (Supplementary Figures S1 and S2). The enzymatic cleavage patterns of the *cspC* 5′UTR illustrated the differences between both structures more clearly than those of the *cspB* 5′UTR. The *cspC* 5′UTR showed an increased sensitivity to RNase S1 and T1 reactivities between nucleotides 7–11, 19–24, 65 and 72 at 37°C while only few RNase cleavages (∼42–43) could be observed at 22°C, indicating that the region comprising the first ∼60–70 nucleotides adopted a double-stranded configuration at such temperature (Supplementary Figure S2). Regarding the *cspB* 5′UTR probing, RNAse S1 cleavage patterns were similar to those found in *cspC*, suggesting that both 5′UTRs might be analogously reorganized in function of temperature changes (Supplementary Figure S1). Note that although several of the RNase T1 processing correlated with the expected structure at the corresponding temperature, there were some minor cleavages that suggested that both structures might coexist at some point *in vitro*. The existence of two alternative structures in each of the *cspB* and *cspC* 5′UTRs indicated that they could also work as thermosensitive RNA elements to control protein expression.

The hairpin of the O conformation acts as a thermoresponsive element

The long hairpin found in the O conformation appeared to be critical for the reorganization of the *cspB* and *cspC* 5′UTR structures. Since it sequestered the anti-RBS region, this would imply that the hairpin would need to unfold itself to release the anti-RBS and block CspB/CspC translation (Figure 3). Seeing that such mechanism would apparently respond to temperature changes, it seemed possible for the hairpin itself to behave as a thermoresponsive element. To explore this further, we used a molecular beacon (MB) system, as previously described (40,48). The MB

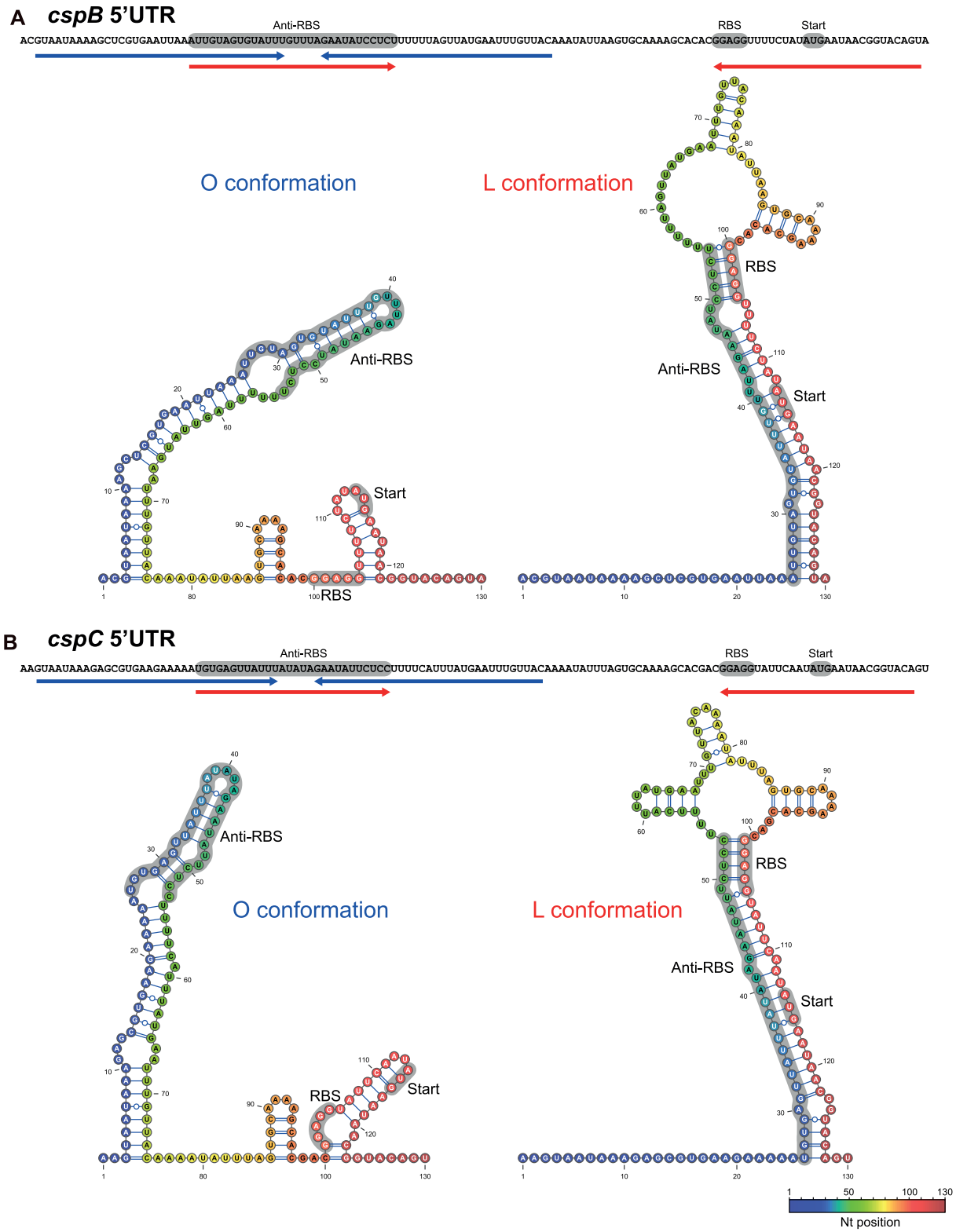

Figure 3. Putative alternative structures adopted by the *cspB* and *cspC* 5′UTRs. RNA structures were predicted using the mfold web server tool (38) and visualized and drawn with the VARNA software (39). Colours represent nucleotide positions within the RNA. Blue and red arrows below the 5′UTR sequences indicate the interacting nucleotide regions in the O and L conformations, respectively. The RBS sequence, the start codon and the anti-RBS region appear as grey shaded areas.

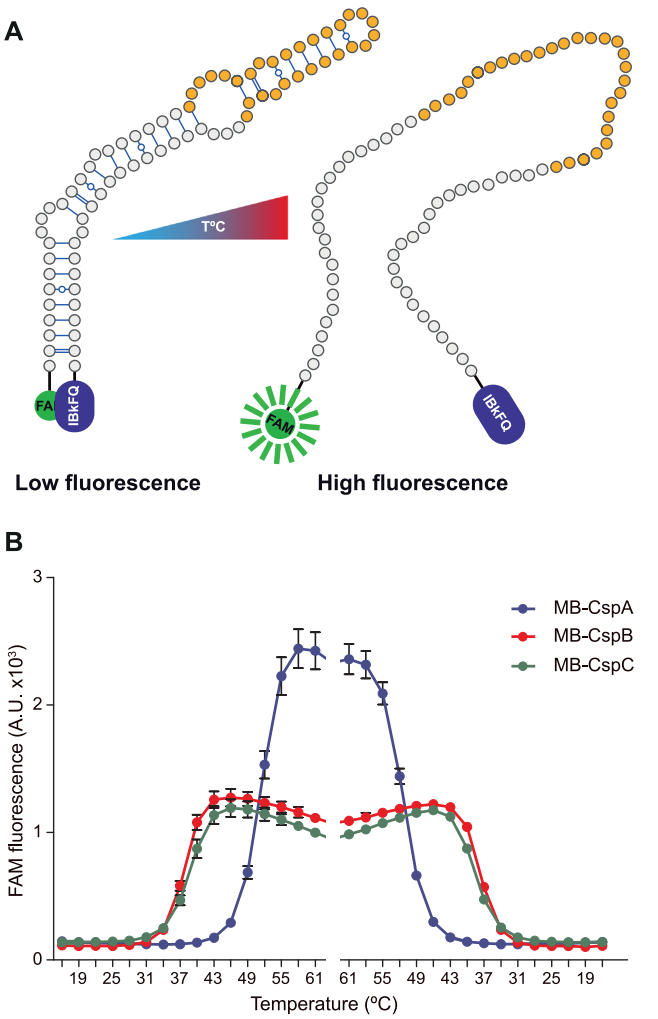

Figure 4. The *cspB* and *cspC* hairpins from the O conformation could work as thermoresponsive RNA elements. (**A**) Schematic representation of the MB design that mimics the stem loop of the O conformation from the *cspB* and *cspC* 5′UTRs. The 5′ and 3′ ends harbour the FAM and IBkFQ molecules, respectively. Fluorescence emission occurs when the FAM fluorophore is separated from the IBkFQ quencher. (**B**) Detection of the FAM fluorescence from MB-CspB (red), MB-CspC (green) and MB-CspA (blue) in function of the temperature. The MBs were equilibrated at 13°C for 10 min and then the temperature was increased 3°C every 5 min. After 5 min of incubation at 65°C, the temperature was gradually decreased following the inverse pattern. Fluorescence was registered for the duration of the experiment. Means and standard deviations from three independent replicates are shown.

consisted of ∼75-mer ssDNA oligonucleotides that were designed to mimic the long hairpin found in the O conformation of the *cspB* and *cspC* 5′UTRs. Additionally, the 5′ and 3′ ends of the oligonucleotides carried the carboxyfluorescein fluorescent dye (FAM) and the IBkFQ quencher, respectively (Figure 4A). If the MB folded at low temperatures as expected, both molecules would fall in close proximity to each other, preventing fluorescence emission (48). We began by incubating the *cspB* and *cspC* MBs at 16°C for 5 min and then increased the temperature in intervals of 3°C every 5 min until 65°C were reached. After 5 min of incubation at 65°C, we gradually decreased the temperature using the same intervals. We monitored the fluorescence emission during the entire process and included the MB that mimicked the *cspA* 5′UTR hairpin as a control (40), since it was not dependent on temperature changes (Figure 1B). The results showed that fluorescence emission could not be registered at 16°C for the *cspB* and *cspC* MBs, indicating that at this temperature they were folded as expected. When reaching temperatures above ∼31°C, FAM fluorescence was registered, with a maximum peak at ∼43°C (Figure 4B). Correspondingly, as the temperature decreased, so did the fluorescence emission and once below 30°C no signal was detected, indicating that the hairpin structures had been restored (Figure 4B). All in all, these results showed that the *cspB* and *cspC* hairpins of the O conformation unfolded at host-related temperatures, which range from 30–33°C (human nose temperature) to 37–41°C (human infection temperature) (10,51). In contrast, the *cspB* and *cspC* MBs were completely folded (no fluorescence emission was detected) when exposed to ambient temperatures (below 30°C). Regarding the *cspA* MB control, it melted and emitted fluorescence when incubated above 43°C, which does not correlate with optimal growth conditions for *S. aureus*. Altogether, these data strongly suggested that the O conformation folds in a temperature-dependent manner, compatible with a model in which the RBSs of *cspB* and *cspC* are sequestered at host temperatures while remaining free at ambient (lower) temperatures.

Mutations in the *cspB* and *cspC* 5′UTRs confirm thermosensitive 5′UTR structural reorganizations *in vivo*

To further validate the predicted alternative 5′UTR structures *in vivo*, we constructed the p5′UTR^{cspB}-*gfp*- and p5′UTR^{cspC}-*gfp*-derived plasmids that included several mutations in the *cspB* and *cspC* 5′UTRs (Supplementary Figure S3). On the one hand, we generated the 5′UTR^{cspB}Δ24-*gfp* and 5′UTR^{cspC}Δ24-*gfp* plasmids, which carried a deletion of the first 24 nucleotides from both 5′UTRs (Supplementary Figure S3). Such nucleotides would be essential to form the long thermoresponsive hairpin of the O conformation (Figure 3). At the same time, this deletion would not hinder the L conformation but rather favour it (Figure 3 and Supplementary Figure S3). In agreement with this, western blot analyses revealed that the GFP expression was drastically reduced in strains expressing the 5′UTR^{cspB}Δ24-*gfp* and 5′UTR^{cspC}Δ24-*gfp* mRNAs (Figure 5). We next performed site-directed mutagenesis in the *cspB* 5′UTR of the p5′UTR^{cspB}-*gfp* plasmid, by replacing nucleotides 47-UAU-49 with AA. Since nucleotides 47-UAU-49 would base pair with nucleotides 33-GUA-35 to form the hairpin structure in the O conformation, such substitution would cause a destabilization and, hence, favour the alternative L conformation (Figure 3 and Supplementary Figure S3). As anticipated, western blot results showed lower GFP levels for the strain carrying the mutated plasmids regardless of the temperature (Figure 5). On the other hand, we substituted 50-C for a G and 55-UU-56 for AA in the *cspB* 5′UTR of p5′UTR^{cspB}-*gfp* and 48-UU-49 by an A in the *cspC* 5′UTR of p5′UTR^{cspC}-*gfp* (Supplementary Figure S3). These mutations would favour the O conformation over the L conformation (Figure 3 and Supplementary Figure S3). Western blot results showed that these *cspB* and *cspC* 5′UTR substi-

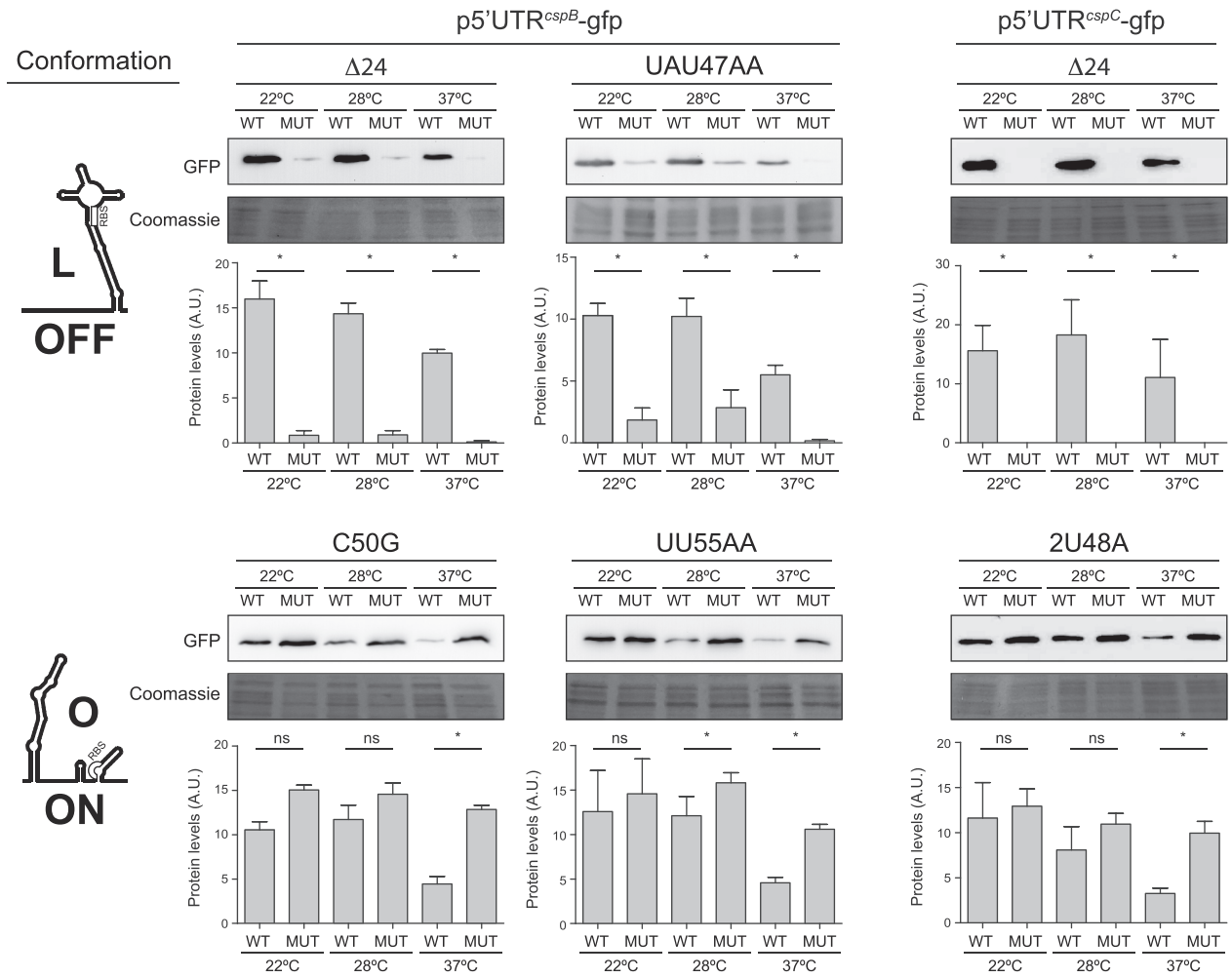

Figure 5. The production of CspB and CspC is controlled by alternative 5′UTR conformations *in vivo*. Western blots showing the effect of different mutations in the 5′UTR of the p5′UTR^{cspB}-*gfp* and p5′UTR^{cspC}-*gfp* plasmids on the GFP levels. Such mutations favoured one of the two 5′UTR alternative conformations. The expected conformation for each mutation, O (translation ON) or L (translation OFF), is indicated on the left hand side of the figure. Coomassie stained gel portions are included as loading controls. Bar plots represent the mean and standard deviation of protein levels from three independent biological replicates, which were determined by densitometry of protein bands using ImageJ (https://imagej.nih.gov/ij/). Asterisks represent statistical significance ($P < 0.05$, Mann–Whitney U test); ns, not significant. Representative images from the triplicates are shown.

tutions led to similar GFP production levels (at all the tested temperatures) to the ones found in the WT p5′UTR^{cspB}-*gfp* and p5′UTR^{cspC}-*gfp* versions at 22°C (Figure 5). This indicated that such nucleotide substitutions made the 5′UTRs unresponsive to temperature changes while highlighting the relevance of alternative *cspB* and *cspC* 5′UTR structures *in vivo* for blocking or facilitating translation in response to temperature shifts.

CspA represses the expression of CspB and CspC in *S. aureus*

Previous results showed that the *E. coli cspA* and *cspB* thermosensors required the action of CSPs to modulate their 5′UTR structures (20). Zhang *et al.* reported that the structural rearrangements did not occur in a Δ*cspABEG* strain, which lacked the *csp* ORFs while retaining their 5′UTRs. In fact, these authors showed that CspA regulated its own production by binding its own mRNA and preventing the formation of a double-stranded *cspA* 5′UTR structure (20). To test whether CspB or CspC participated in the structural reorganizations of their own 5′UTR thermosensors and, therefore, autoregulated their production, we electroporated the translational reporter plasmids p5′UTR^{cspB}-*gfp* and p5′UTR^{cspC}-*gfp* into the *S. aureus* Δ*cspB* and Δ*cspC* strains, respectively. Western blot results showed a similar behaviour in terms of GFP expression between the WT and mutant strains for all the tested temperatures (Supplementary Figure S4). This indicated that the production of both proteins was not autoregulated, at least in the tested conditions. Previous CspA co-immunoprecipitation studies from our group showed that CspA was able to bind the *cspB* and *cspC* mRNAs *in vivo*. Deletion of *cspA* increased CspC production, indicating that the regulation of CSPs is interconnected in *S. aureus* (40). To corroborate these results and analyse whether CspA also modulated CspB expression, we deleted the *cspA* gene from the strains expressing the chromosomally tagged CspB^{3xF} and CspC^{3xF} proteins and performed western blots. Figure 6A shows that deletion of the *cspA* gene increased the CspB^{3xF} and CspC^{3xF} protein levels at 37°C, confirming its role in the regulation process (Fig-

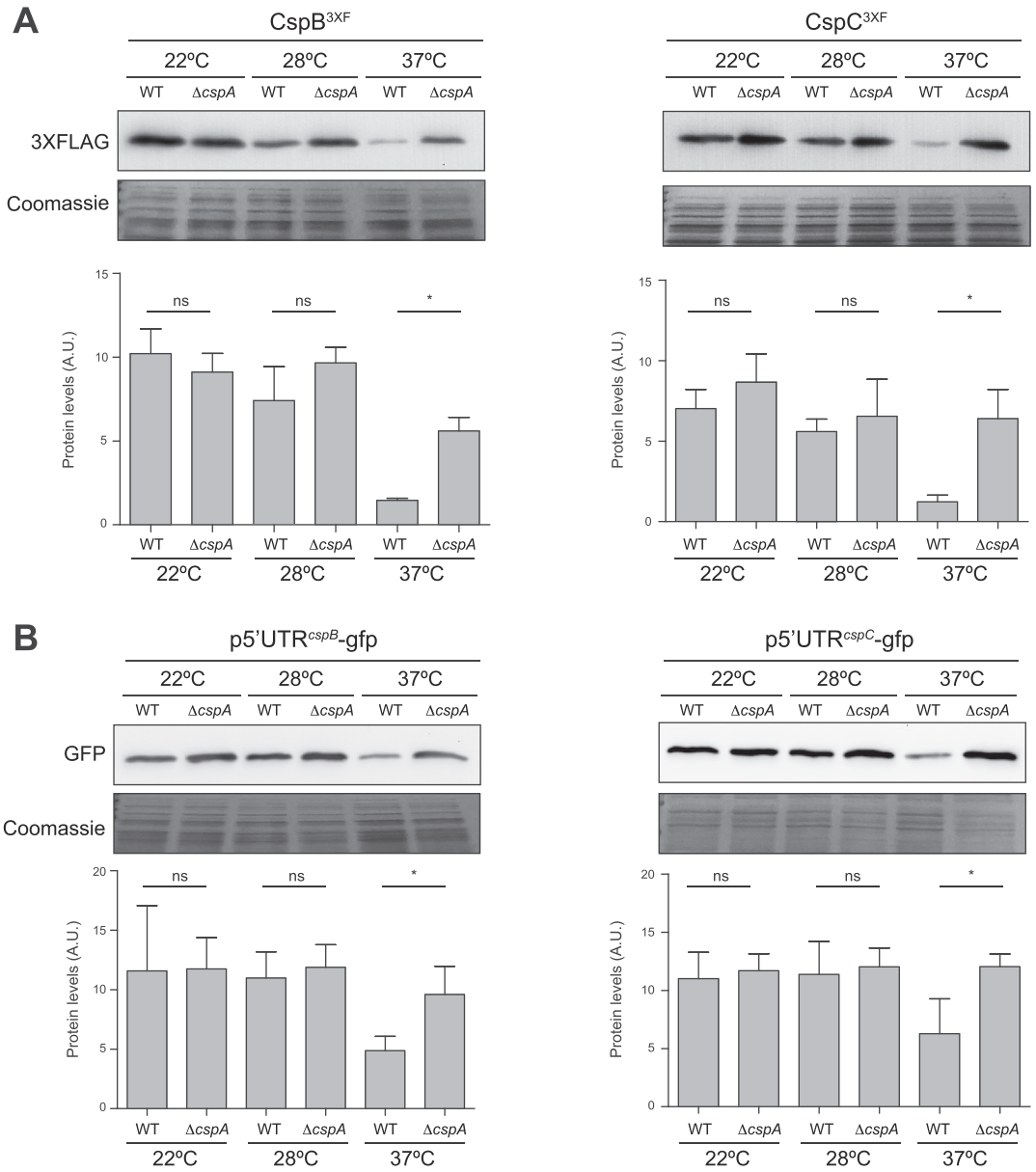

Figure 6. CspA participates in repressing the production of CspB and CspC at 37°C. (**A**) Western blot showing the chromosomal expression of CspB^{3xF} and CspC^{3xF} from the WT and Δ*cspA* strains grown in MH broth at 22, 28 and 37°C. (**B**) Western blot results of the GFP levels expressed from the *S. aureus* WT and Δ*cspA* strains, carrying the *cspB* and *cspC* 5′UTR-GFP translational reporter plasmids after growth in MH broth at 22, 28 and 37°C. The 3xFLAG-tagged proteins and GFP signals were developed as described in Figures 1 and 2, respectively. Coomassie stain gel portions are included as loading controls. Bar plots represent the mean and standard deviation of protein levels from three independent biological replicates, which were determined by densitometry of protein bands using ImageJ (https://imagej.nih.gov/ij/). Asterisks represent statistical significance ($P < 0.05$, Mann–Whitney *U* test); ns, not significant. Representative images from the triplicates are shown.

ure 6A). We then analysed whether CspA might participate in the thermoregulation of CspB and CspC through their 5′UTR regions. To test this, we electroporated the translational reporter plasmids p5′UTR^{cspB}-*gfp* and p5′UTR^{cspC}-*gfp* in the *cspA* mutant and performed western blot experiments. The GFP levels in the Δ*cspA* mutant were higher than those in the WT strain when grown at 37°C, confirming that CspA repressed CspB and CspC through their 5′UTRs. When strains were grown at 22 and 28°C, no significant GFP differences were found (Figure 6B). Altogether, these results confirmed that CspA repressed CspB and CspC production probably by interacting with the *cspB* and *cspC* 5′UTRs.

CspA represses CspB and CspC by favouring the L conformation at 37°C

To gain further insight into how CspA regulates CspB and CspC, we considered two hypotheses: (1) CspA would directly bind the RBS and block translation, or (2) CspA would interact with the 5′UTR and favour the L conformation, repressing *cspB* and *cspC* mRNA translation. To

test these hypotheses, we electroporated the *cspA* mutant with the translational reporter plasmids carrying all the above-mentioned 5′UTR mutations (Supplementary Figure S3). We then compared the GFP levels in the Δ*cspA* reporter strains grown at 37°C with those of their WT counterparts by western blot (Figure 7). We found no significant differences between the GFP expression levels in the WT and Δ*cspA* strains carrying the 5′UTR mutants that favour the O conformation (C50G and UU55AA in *cspB* 5′UTR and UU48A in *cspC* 5′UTR) (Figure 7A and B). This suggested that CspA could not inhibit CspB/C expression when the RBS became more accessible. Moreover, no differences were found when comparing the GFP levels of the WT and Δ*cspA* strains carrying the reporter plasmids that favoured the L conformation (p5′UTR^{cspB}Δ24-*gfp* and p5′UTR^{cspC}Δ24-*gfp*) (Supplementary Figure S3 and Figure 7A and B). This indicated that CspA was dispensable for repression when forcing the L conformation by deleting the first 24 nucleotides. We only found a slight but significant increase in the GFP expression from the Δ*cspA* strain carrying the *cspB* UAU47AA mutation (Figure 7A), which promoted the L conformation by simultaneously destabilizing the hairpin of the O conformation (Figure 3 and Supplementary Figure S3). This may indicate that destabilizing the O conformation favours the CspA repression effect. However, it may also be possible for CspA to be sensitive to 5′UTR mutations that cause changes in the nucleotide-pairing affinity. It has been proposed before that CSPs bind RNA weakly and in a non-specific way. However, in some occasions, certain RNA motifs could contribute to CSP functionality (40,52–54). For example, we showed that the autoregulation of CspA in *S. aureus* requires a U-rich motif located in the *cspA* 5′UTR (40). Notably, the *cspB* 5′UTR carries several U-rich motifs (Figure 3), two of which (36-UUUGUUU-42 and 54-UUUUUU-59) are involved in the folding of the O conformation. Additionally, motif 36-UUUGUUU-42 participates in the nucleotide pairing of the L conformation (Figure 3). It could be possible for CspA to target these regions at 37°C to prevent the folding of the O conformation. Note that validations *in vivo* turned out to be extremely difficult because the 5′UTR mutants in these potential CspA binding sites could not be constructed without affecting the folding of both alternative conformations. When comparing both U-rich regions, the second motif (54-UUUUUU-59) presented more unpaired bases in either of the two conformations than the first one. Therefore, we chose this region to examine the role of U-rich motifs in the regulation of *cspB* by CspA (Figure 3). To analyse whether the increased reporter expression observed in the UU55AA mutant (Figure 7A) was due to changes in the folding affinities and/or due to the inability of CspA to bind a mutated 54-UUUUUU-59 target motif, we generated an additional mutation (UU26AA; nucleotides 26-UU-27 substituted by AA) in the UU55AA mutant that reconstituted the hairpin bubble (Figures 3 and 7C). As a control, we also constructed the UU26AA mutant in the *cspB* 5′UTR (Figure 7C). Western blot experiments showed that CspA repressed the GFP reporter translation in the double UU55AA/UU26AA mutant (Figure 7D). This suggested that motif 54-UUUUUU-59 was dispensable for CspA to exert its repression. Next, we focused on the other U-rich motif (36-UUUGUUU-42) and generated an additional mutant (36-UUCGUCU-42) (Figure 7E). Note that these nucleotide changes were intended to avoid any significant variations in both conformations (O and L) (Figures 3 and 7E). Western blot results revealed that when we introduced the plasmid harbouring this mutation in the WT strain, the GFP levels increased and reached similar levels to the ones present in the Δ*cspA* strain (Figure 7D). This result suggested that CspA repressed CspB production by interacting with the *cspB* mRNA through the 36-UUUGUUU-42 motif. Altogether our data lead to a functional model in which CspA binds the loop of the distal stem of the O conformation and favours the L conformation that represses CspB translation at 37°C.

Thermoregulation of CSPs is required for *S. aureus* adaptation to ambient temperatures

Besides its pathogenicity, the ability to colonize different niches as well as to spread rapidly by direct contact and/or through contaminated surfaces make *S. aureus* a life-threatening pathogen (10). The higher CspB and CspC protein expression at ambient temperatures suggested that these proteins could contribute to *S. aureus* adaptation when it leaves the host. To further investigate this, we plated serial dilutions of overnight cultures of the WT and isogenic Δ*cspB* and Δ*cspC* mutant strains in TSA plates and incubated them at 22 and 37°C. As shown in Figure 8A, we found no growth differences between the WT and *csp* mutants at the tested temperatures. Since both CSPs were induced at ambient temperatures (Figure 1B), it seemed possible for these proteins to play redundant roles, as previously described in *E. coli* and *B. subtilis* (19,24,55,56). To address this issue, we generated a double mutant strain (Δ*cspBC*) and analysed its growth at different temperatures. Interestingly, we observed a significant growth deficiency at 22°C when compared with the WT strain (Figure 8A). This result suggested a biological redundancy between CspB and CspC as the double deletion attenuated the ability of *S. aureus* to grow at low temperatures.

In order to evaluate the biological relevance of the thermoregulation mechanism controlling CspB and CspC expression, we constructed chromosomal mutants that modified the structural organization of the 5′UTR to prevent *cspB* and *cspC* mRNA translation. Out of the different mutations shown in Supplementary Figure S3, we chose to delete the first 24 nucleotides from both *cspB* and *cspC* mRNAs since these mutations produced the strongest GFP repression in our previous constructs (Figure 5). First, to control that these mutations produced the same effect in the chromosome as seen for the reporter plasmids, the corresponding 24 nt were deleted from the tagged *cspB*^{3xF} and *cspC*^{3xF} strains. We performed western blot analyses and confirmed that the chromosomal Δ*24B*^{3xF} and Δ*24C*^{3xF} mutant strains were not able to produce CspB^{3xF} and CspC^{3xF} (Figure 8B). Analogously, we studied *cspB* and *cspC* mRNA levels through northern blots (Supplementary Figure S5A). The Δ24 deletion produced no significant variations on the *cspB*Δ*24*^{3xF} mRNA levels when compared to the WT mRNA. On the contrary, the *cspC*Δ*24*^{3xF} mRNA levels were significantly lower than those of the

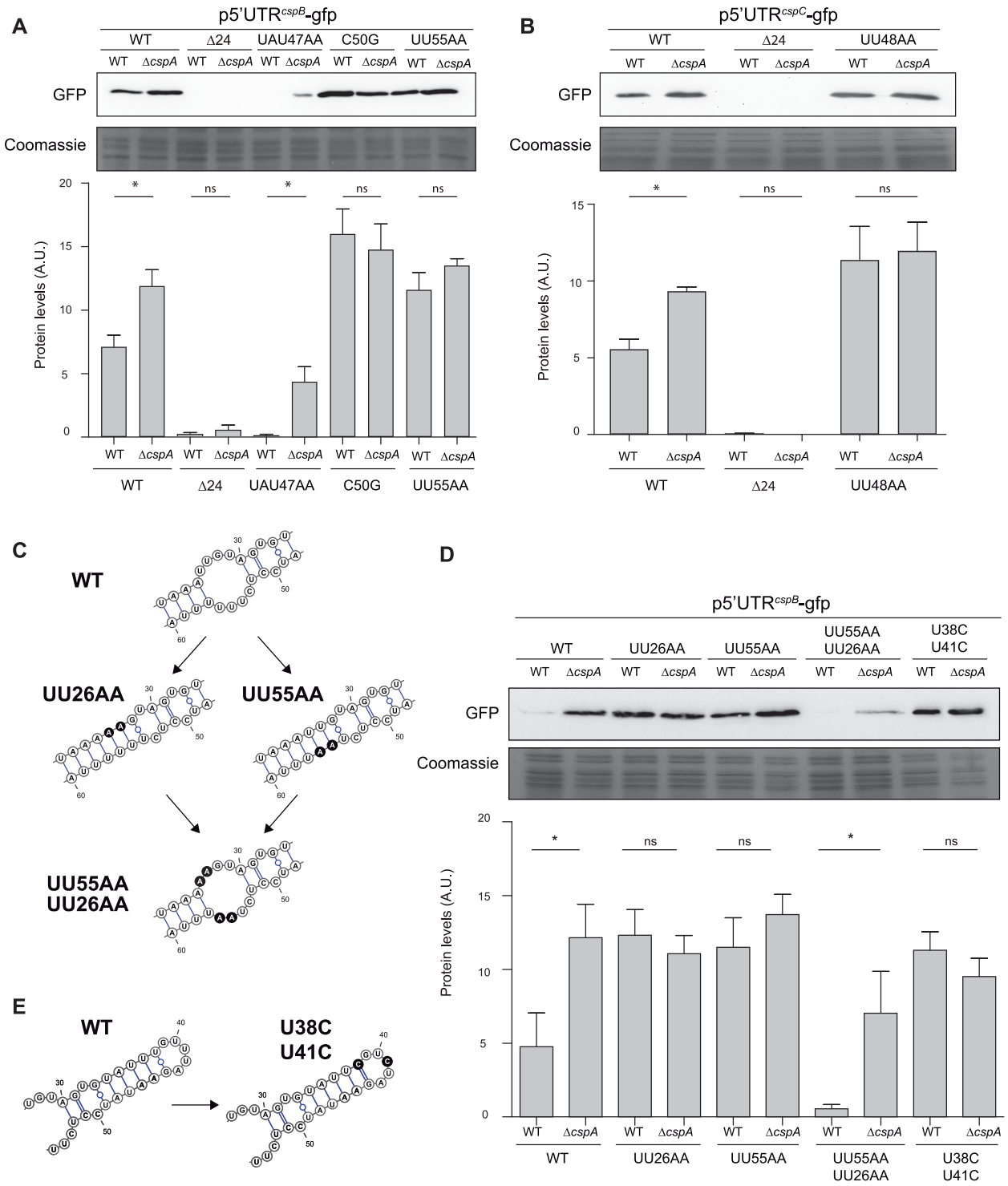

Figure 7. CspA is required for promoting the L conformation at 37°C and repressing CspB and CspC production. (**A**, **B** and **D**). Western blots showing the GFP levels from the WT and Δ*cspA* strains expressing the WT and mutated *cspB* or *cspC* 5′UTR-GFP reporter plasmids. Total protein extracts were processed as described in Figure 2. Coomassie gel portions are included as loading controls. Bar plots represent the mean and standard deviation of the GFP levels from three independent biological replicates, which were determined by densitometry of protein bands using ImageJ (https://imagej.nih.gov/ij/). Asterisks represent statistical significance ($P < 0.05$, Mann–Whitney U test); ns, not significant. Representative images from the triplicates are shown. (**C** and **E**). Schematic representations of the mutations introduced in the *cspB* 5′UTR. The substituted nucleotides are shaded in black.

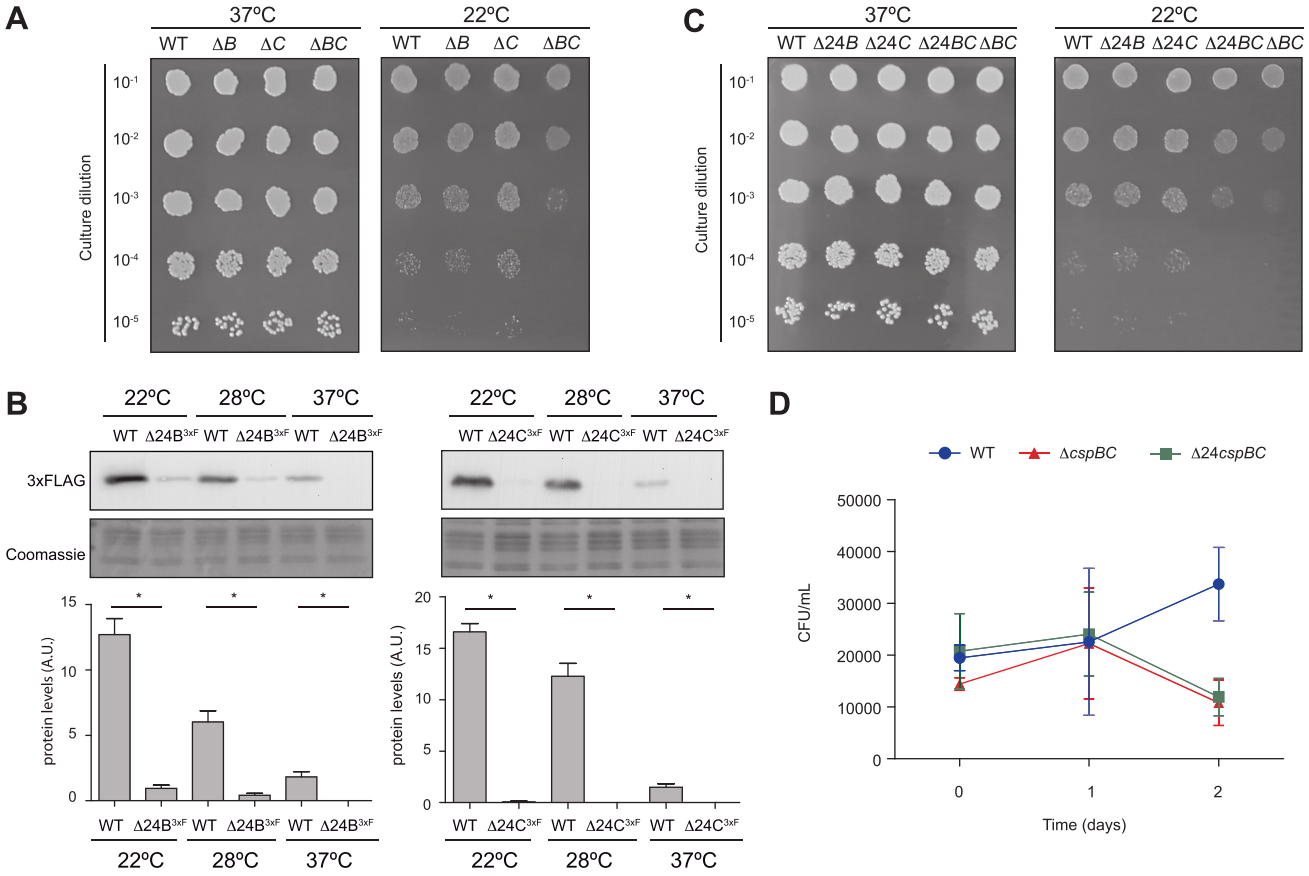

Figure 8. Simultaneous mutations in CspB and CspC RNA thermoswitches affect *S. aureus* growth at ambient temperatures. (**A** and **C**) Growth assay at 37 and 22°C of the different *csp* mutants. Bacteria were grown at 37°C and 200 rpm overnight and diluted to an OD_{600nm} of 1. Ten-fold dilutions were plated in TSA plates and incubated at 37 and 22°C for 24 and 72 h. A representative image from three independent biological replicates is shown. (**B**) Western blot showing the expression of the 3xFLAG-tagged CspB and CspC proteins from the Δ24B and Δ24C mutants, which were grown at the indicated temperatures. Protein extraction and western blots were performed as previously described in Figure 1. Coomassie gel portions are included as loading controls. Bar plots show the mean and standard deviation of protein levels from three independent biological replicates, which were determined by densitometry of protein bands using ImageJ (https://imagej.nih.gov/ij/). Asterisks represent statistical significance ($P < 0.05$, Mann–Whitney *U* test); ns, not significant. Representative images from the triplicates are shown. (**D**) Assay mimicking the conditions that *S. aureus* might face when away from the host. A preinoculum was grown in TSB at 37°C and 200 rpm overnight. Bacteria were then washed, diluted 1:250 and regrown at 32°C and 200 rpm for 2 days in SNM3, resembling the nasal state. To imitate fomite contamination, bacteria were transferred to fresh SNM3 and incubated at 22°C. CFUs were counted 0, 1 and 2 days after incubation at 22°C. The plot represents the results from at least three independent replicates.

cspC^{3xF} WT mRNA. A similar behaviour was observed for the WT and Δ24 *cspB* and *cspC* 5′UTRs-*gfp* translational reporter fusion mRNAs (Supplementary Figure S5B). On the one hand, this result suggested that the decreased *cspC* mRNA expression observed in the Δ24 deletion was not caused by a putative *cspC* promoter activity disruption. Note that the reporter fusions were expressed from a constitutive heterologous promoter. On the other hand, the results indicated that the Δ24 deletion produced different outputs for the *cspB* and *cspC* mRNA levels. Whether this was a consequence of forcing the L conformation or because of a change in the mRNA stability without any functional meaning remains unanswered. Interestingly, this leaves room for speculation on how the subtle differences between such apparently similar orthologous regulatory 5′UTRs may lead to different outcomes and, perhaps, explain the need for both genes to coexist in the same genome. Regardless, the Δ24 deletions produced the expected decrease in the production of both CspB and CspC proteins and led us to engage into phenotypic analysis. Therefore, the same mutations were performed in the WT strain to create the single mutants Δ*24B* and Δ*24C* and the double mutant Δ*24B*–Δ*24C*. Overnight cultures of these strains were diluted and plated on TSA plates. As observed for the single *cspB* and *cspC* gene mutations, the Δ*24B* and Δ*24C* 5′UTR deletions did not affect *S. aureus* growth at ambient temperatures. In contrast, the double Δ*24B*–Δ*24C* mutant strain presented a growth defect comparable to the Δ*cspBC* mutant when incubated at 22°C (Figure 8C). This result confirmed that the *cspB* and *cspC* 5′UTR thermoregulation was required for CspB and CspC production and, therefore, critical for *S. aureus* efficient growth at ambient temperatures.

Considering that one of the major reservoirs of *S. aureus* in the human body is the nose and that *S. aureus* is often disseminated through human nasal secretions that contaminate diverse fomites (9), we recreated such scenario by growing the WT, Δ*24B*–Δ*24C* and Δ*cspBC* strains in Erlenmeyer flasks containing SNM3 for 2 days at 32°C and

220 rpm. SNM3 reproduces the composition of nasal secretions (49), 32°C is the temperature found in the nose (51) and agitation (220 rpm) favours aeration. After this incubation period, no growth differences were observed among the strains. Then, the bacterial cultures were normalized to an OD_{600nm} of 0.05 using fresh SNM3 and transferred to new sterile flasks. The WT and mutant strains were incubated for 48 h at 22°C without shaking to mimic the transition between the nasal and the fomite state through mucus secretion. The number of viable *S. aureus* cells was then estimated by counting the CFUs per millilitre on TSA plates at different time points. As shown in Figure 8D, whereas the WT strain replicated in SNM3 at 22°C, the Δ*24B*–Δ*24C* and Δ*cspBC* mutant strains showed a significant growth defect after 48 h of incubation. Altogether, these data demonstrated that CspB and CspC thermoregulation is required for *S. aureus* adaptation and survival at ambient conditions, a scenario that this pathogen may face when it leaves its natural host.

The existence of alternative 5′UTR *csp* structures may apply to other bacteria

In order to analyse whether the above mentioned thermoswitch mechanism might be conserved among other bacterial species, we performed blastn analyses using the first 127 nucleotides of the *cspB* mRNA as a query in the Microbes NCBI website (https://blast.ncbi.nlm.nih.gov/Blast.cgi). The results showed that >50 *csp* genes from 43 different *Staphylococcus* species carried an orthologous *cspB* 5′UTR. The sequences were highly conserved, with an identity >74% (Supplementary Table S4). The number of CSPs among the analysed staphylococcal species was variable, ranging from 1 to 3 (36). In most of the *Staphylococcus* genomes containing three *csp* genes, two of them harboured 5′UTRs similar to *S. aureus cspB*/*C* 5′UTRs. However, among the genomes with two *csp* genes, only one of them carried a putative thermoswitch (Supplementary Table S4). In the case of *Staphylococcus pettenkoferi* and *Staphylococcus kloosii*, whose genomes contained just one *csp* gene, the 5′UTR sequence was significantly different from the *S. aureus cspB* 5′UTR. This might be explained by the fact that their CSP showed a high degree of identity with *S. aureus* CspA protein (36).

Multiple sequence alignments also revealed that the nucleotides required for adopting the alternative conformations were highly conserved among staphylococcal species (Supplementary Figures S6 and S7). Although the *cspB*/*C* 5′UTR sequence conservation was not preserved beyond the *Staphylococcus* genus, the fact that orthologous thermoswitch mechanisms had been previously found in *E. coli* and *L. monocytogenes* (20,28,33) indicated that the thermoregulation of CSPs based on mutually exclusive alternative 5′UTR conformations could be a common regulatory mechanism in bacteria. Since bacterial genomes often encode several CSP paralogues with a high protein identity, it might be difficult to predict which CSPs are involved in cold adaptation without further experimentation. Although the *csp* 5′UTRs might not share a high sequence identity with the RNA thermoswitches described so far, the existance of alternative structures could be an indicator of such function. To validate this idea, we looked for putative alternative conformations in the 5′UTRs of all the *csp* genes from representative bacteria such as *Enterococcus faecalis*, *B. subtilis*, *Clostridium perfringens*, *Salmonella enterica* sv Typhimurium and *Pseudomonas aeruginosa* (Supplementary Table S5). Since the already identified thermoswitches were located within 5′UTRs with lengths ranging from 110 to 160 nt, query sequences including at least 120 nt upstream of the start codon of each CSP were selected to predict putative secondary structures using the mfold web server (38). According to preliminary predictions, query sequences were enlarged or shortened to look for alternative folding options. Thus, we identified several putative *csp* 5′UTRs that displayed alternative structures resembling the ones previously described (Supplementary Table S5 and Figure 9). For example, we predicted putative RNA thermoswitches in two out of the six *csp* genes from *E. faecalis*, *S. enterica* sv Typhimurium and *P. aeruginosa*, whereas one was predicted in *C. perfringens* and *B. subtilis* (Supplementary Table S5). On the one hand, these results indicated that the alternative conformations of *csp* 5′UTRs may be a conserved regulatory feature in bacteria despite lacking significant sequence similarity. On the other hand, structural predictions could help identifying CSPs whose expression may be post-transcriptionally controlled by alternative RNA conformations.

DISCUSSION

RNA-mediated thermoregulation is an essential process that promotes changes in gene expression and facilitates the adaptability of pathogenic bacteria when they transition from the host to the environment and vice versa. Several RNA thermosensors have been found to induce the expression of main regulators required for the activation of virulent genes in bacteria while infecting humans. Throughout this process, the zipper-like structures located at the 5′UTR of genes required for survival inside the host sense an increase in the temperature and unfold, which in turn releases the otherwise blocked RBSs. In this manner, they become accessible to the ribosomes for translation initiation (57–63). Conversely, a few RNA thermosensors have been identified as capable of activating gene expression upon drops in the temperature (20,28,33). In comparison with regular zipper-like RNA thermosensors, activation of translation at lower temperatures involves much more complex RNA structural reorganizations.

In this study, we demonstrated that *S. aureus* adapts to low temperatures by modulating CspB and CspC expression. The CspB and CspC thermoregulation occurred at the post-transcriptional level through the action of two thermosensitive RNA elements located at the 5′UTR of the *cspB* and *cspC* mRNAs, respectively (Figure 3). These thermosensors induced CspB and CspC translation at ambient temperatures while repressing it at host-related temperatures (Figure 2). By using conditions that mimicked the *S. aureus* nasal and fomite contamination, we demonstrated the importance of RNA-mediated thermoregulation for the survival of such bacterium in the environment. Chromosomal deletions of the first 24 nucleotides of the *cspB* and *cspC* mRNAs (Δ24*BC* strains) eliminated the transitions

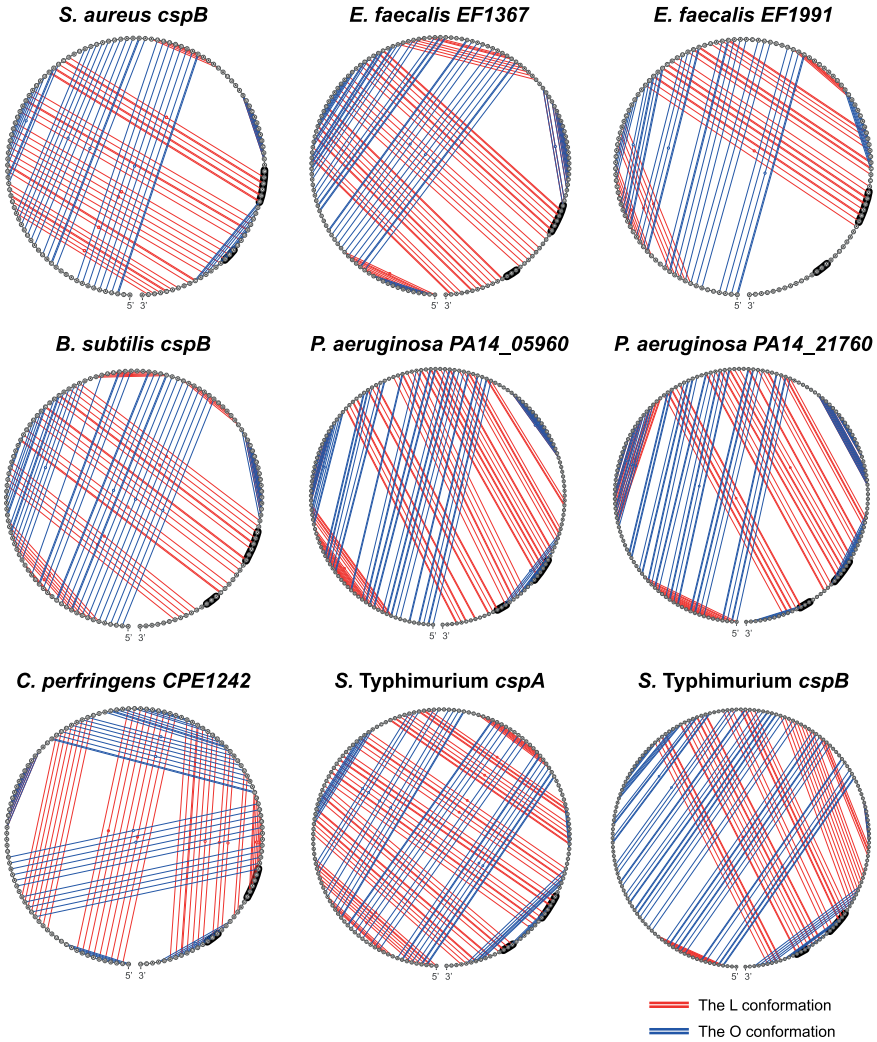

Figure 9. RNA alternative conformations are widely spread in *csp* genes of several bacteria. Circular structural representation of alternative RNA secondary structures found in the 5′UTRs of the *csp* mRNAs from *E. faecalis*, *B. subtilis*, *C. perfringens*, *S. enterica* sv Typhimurium and *P. aeruginosa.* The 5′UTR secondary structure of *cspB* from *S. aureus* is included as a control. Blue and red lines represent the pairings between nucleotides in the O and L conformations, respectively.

between the two alternative RNA conformations by forcing the folding of the 5′UTR into the L variant. This impaired *S. aureus* growth at 22°C (Figure 8), a similar growth defect to the one observed for the double *cspB* and *cspC* mutant.

Upon further inspection, we found the thermosensitive structural shifts to be orthologous to the ones recently described for *E. coli* and *L. monocytogenes cspA* mRNAs (20,33). These type of RNA structural rearrangements, which repress translation at higher temperatures while activating it at lower temperatures, are also present in the 5′UTR of the bacteriophage *cIII* gene (64). Recently, regulatory 5′UTRs that activate the expression of the holin-like protein CidA at low temperatures have been described for *S. aureus* (65). Hussein *et al*. propose that the *cidA* gene is transcribed by two alternative promoters, generating two different 5′UTRs of 36 and 82 nt, respectively. Translational reporter fusions revealed that both 5′UTRs post-transcriptionally activated CidA translation at low temperatures, the longer *cidA* 5′UTR being the one responsible for the highest CidA protein expression. Other than the closed conformation identified by Hussein *et al*. (65), we could also predict by mfold a putative alternative conformation in the longer *cidA* 5′UTR that would make the RBS available to the ribosome at low temperatures (Supplementary Figure S8). This open conformation would involve a long hairpin comprising nucleotides 5–66 of the *cidA* 5′UTR that would sequester the anti-RBS motif (Supplementary Figure S8), resembling the mechanism found for CspB and CspC. It would be interesting to investigate which are the signals responsible for the activation of each of the *cidA* alternative promoters.

Altogether, these examples indicated that the thermoregulatory mechanism based on RNA conformational switches could be widely extended. In agreement with this idea, we were able to predict orthologous *cspB* thermosensors in all *Staphylococcus* species, with the exception of *S. pettenkoferi* and *S. kloosii*, whose genomes only encoded CspA. Note

that CspA expression was not affected by temperature shifts in *S. aureus*.

Considering that multiple *csp* genes are present in the core genome of most bacteria, one would expect this type of RNA thermoswitch to be distributed beyond sequence conservation. In fact, we found that orthologous alternative structures could also be predicted in the 5′UTRs of *csp* mRNAs from several representative bacteria, including *E. faecalis*, *B. subtilis*, *C. perfringens*, *S. enterica* sv Typhimurium and *P. aeruginosa* (Figure 9). Moreover, examples like the *cIII* and *cidA* thermosensors indicated that these regulatory elements may not be restricted to the *csp* gene family (64,65).

Although the *cspB* and *cspC* 5′UTR structures significantly differ from the regular RNA thermosensors (11,32,63), the hairpin of the O conformation seems to work like the already known zipper-like structures. However, the outcome of this mechanism is rather different as instead of freeing the RBS when melting, it is the anti-RBS region that is released. Therefore, in addition to masking RBSs or anti-RBSs, it could be speculated that bacterial genomes may encode alternative thermosensitive hairpins that may also sequester other binding sites for ribonucleases, RNA-binding proteins and/or non-coding RNAs, making such motifs available or unavailable depending on the environmental temperature.

In agreement with previous results from *E. coli* and *B. subtilis* studies, we showed that besides from shifts in the temperature, *S. aureus cspB* and *cspC* genes can also be negatively regulated by a *csp* paralogue (20,24,55). In *E. coli*, CspA downregulates the expression of CspB, CspE and CspG proteins (55). Additionally, in *B. subtilis* the lack of one member of the CSP family produces the upregulation of the others, suggesting that CSPs control is interconnected (24). Previous RNA immunoprecipitation experiments from our group showed that the *cspB* and *cspC* mRNAs were targeted by CspA in *S. aureus* (40). Here, we propose CspA as an essential player that favours the L conformation over the O conformation at 37°C (Figure 7). Although CspA regulates its own expression in *S. aureus* by preventing the folding of a long hairpin in the *cspA* 5′UTR (40), such hairpin is unsensitive to physiological temperatures (Figure 1). Since CspA levels remain unaltered upon temperature changes, it is difficult to explain how CspA can repress CspB/C translation on its own (Figure 1). We reasoned that if it takes part in regulating both of its paralogues, it should work in conjunction with temperature-dependent elements. CspA seems to interact with one of the U-rich motifs located at the 5′UTRs. Specifically, mutations in the *cspB* 36-UUUGUUU-42 motif abolished CspA repression (Figure 7). Interestingly, this motif is located at the top of the hairpin that is unfolded when temperature increases (Figure 4). This interaction would prevent the folding of the long hairpin in the O conformation at 37°C and allow the anti-RBS to base pair with the RBS in the L conformation. In agreement with this, our *in vivo* experiments showed how deleting the *cspA* gene increased CspB and CspC expression at 37°C (Figure 6). On the contrary, when testing the effect of the presence/absence of CspA on the expression of CspB and CspC at 22°C no significant differences were found. In other words, there was not a temperature-dependent repression of CspB and CspC expression in the absence of CspA. This could be explained by the fact that the RNA secondary structures are more rigid at lower temperatures (20). The affinity between the RNA regions forming the hairpin of the O conformation at 22°C is probably higher than their affinity for CspA. Therefore, it would seem that CspA cannot disrupt the folding of such hairpin at ambient temperatures. We further confirmed this by performing site-directed mutations in the 5′UTRs that altered the affinities of the different RNA regions between them (Figure 5). In most cases, thermoregulation was eliminated and, although it cannot be excluded that some of these mutations could also modify the accessibility of CspA to their binding site, we suggest the thermoregulatory mechanism to be based on the different affinities of the distinct elements involved. These affinities would be naturally altered by temperature shifts.

It remains to be elucidated whether CspB and CspC are functionally redundant in a mechanistic way. Previously, functional redundancy was found among *E. coli*, *Salmonella* and *B. subtilis* CSPs (19,24,55,56). However, we recently showed that the phenotypes of a *cspA* mutant could not be restored by the expression of the CspB or CspC proteins despite their high protein identity, suggesting a certain functional specificity for *S. aureus* CSPs. The CspA specificity related to SigB-associated phenotypes was concentrated in proline 58 of the CspA protein (36). Interestingly, amino acids occupying the same position (58) in the CspB and CspC were different (note that all *S. aureus* CSPs are 66 amino acids long). It is possible that, despite their similarities, *S. aureus* CSPs have different preferences when it comes to sequence affinities, as previously described for *E. coli* and *Salmonella* CSPs (53,56). Determination of the RNA targetomes would help elucidating how CspB and CspC participate on regulating gene expression when *S. aureus* grows at low temperatures.

In summary, our study unveils the thermoregulatory mechanism that controls the expression of CspB and CspC upon temperature shifts. The biological relevance of this thermoregulation is highlighted by the fact that it is required for *S. aureus* optimal growth and survival in ambient conditions. Moreover, we propose the CSP regulation based on RNA alternative conformations to be widely spread in bacteria.

DATA AVAILABILITY

Any data or material that support the findings of this study can be made available by the corresponding author upon request.

SUPPLEMENTARY DATA

Supplementary Data are available at NAR Online.

ACKNOWLEDGEMENTS

We thank Prof. Cristina Solano for critical reading of this manuscript, Anne-Catherine Helfer for excellent technical assistance in probing experiments and Dr Emanuelle Charpentier for pCN51 plasmid (ref. NR-46149), which was

provided by the Network on Antimicrobial Resistance in *Staphylococcus aureus* (NARSA) for distribution by BEI Resources, NIAID, NIH. We acknowledge support of the publication fee by the CSIC Open Access Publication Support Initiative through its Unit of Information Resources for Research (URICI).

FUNDING

A.T.-A. was supported by the European Research Council under the European Union's Horizon 2020 research and innovation program [ERC-CoG-2014-646869]; and the Spanish Ministry of Science and Innovation [PID2019-105216GB-I00] grants. I.C. was supported by Centre National de la Recherche Scientifique (CNRS) through an International Project of Scientific Cooperation between CNRS and CSIC [PICS07507]; and by the framework of the labEx Net RNA, French National Research Agency [ANR-10-LABX-0036 and IMCBio ANR-17-EURE-0023]. Funding for open access charge: CSIC Open Access Publication Support Initiative, Unit of Information Resources for Research (URICI).
Conflict of interest statement. None declared.

REFERENCES

1. Uhlemann,A.C., Knox,J., Miller,M., Hafer,C., Vasquez,G., Ryan,M., Vavagiakis,P., Shi,Q. and Lowy,F.D. (2011) The environment as an unrecognized reservoir for community-associated methicillin resistant *Staphylococcus aureus* USA300: a case-control study. *PLoS One*, **6**, e22407.
2. Scott,E. and Bloomfield,S.F. (1990) The survival and transfer of microbial contamination via cloths, hands and utensils. *J. Appl. Bacteriol.*, **68**, 271–278.
3. Kramer,A., Schwebke,I. and Kampf,G. (2006) How long do nosocomial pathogens persist on inanimate surfaces? A systematic review. *BMC Infect. Dis.*, **6**, 130.
4. Neely,A.N. and Maley,M.P. (2000) Survival of enterococci and staphylococci on hospital fabrics and plastic. *J. Clin. Microbiol.*, **38**, 724–726.
5. Walther,B.A. and Ewald,P.W. (2004) Pathogen survival in the external environment and the evolution of virulence. *Biol. Rev. Camb. Philos. Soc.*, **79**, 849–869.
6. Knox,J., Uhlemann,A.C. and Lowy,F.D. (2015) *Staphylococcus aureus* infections: transmission within households and the community. *Trends Microbiol.*, **23**, 437–444.
7. David,M.Z. and Daum,R.S. (2010) Community-associated methicillin-resistant *Staphylococcus aureus*: epidemiology and clinical consequences of an emerging epidemic. *Clin. Microbiol. Rev.*, **23**, 616–687.
8. Davis,M.F., Iverson,S.A., Baron,P., Vasse,A., Silbergeld,E.K., Lautenbach,E. and Morris,D.O. (2012) Household transmission of meticillin-resistant *Staphylococcus aureus* and other staphylococci. *Lancet Infect. Dis.*, **12**, 703–716.
9. Wertheim,H.F.L., Melles,D.C., Vos,M.C., van Leeuwen,W., van Belkum,A., Verbrugh,H.A. and Nouwen,J.L. (2005) The role of nasal carriage in *Staphylococcus aureus* infections. *Lancet Infect. Dis.*, **5**, 751–762.
10. Tong,S.Y.C., Davis,J.S., Eichenberger,E., Holland,T.L. and Fowler,V.G. (2015) *Staphylococcus aureus* infections: epidemiology, pathophysiology, clinical manifestations, and management. *Clin. Microbiol. Rev.*, **28**, 603–661.
11. Klinkert,B. and Narberhaus,F. (2009) Microbial thermosensors. *Cell. Mol. Life Sci.*, **66**, 2661–2676.
12. Schumann,W. (2012) Thermosensor systems in eubacteria. *Adv. Exp. Med. Biol.*, **739**, 1–16.
13. Lam,O., Wheeler,J. and Tang,C.M. (2014) Thermal control of virulence factors in bacteria: a hot topic. *Virulence*, **5**, 852–862.
14. Onyango,L.A., Hugh Dunstan,R., Roberts,T.K., Macdonald,M.M. and Gottfries,J. (2013) Phenotypic variants of staphylococci and their underlying population distributions following exposure to stress. *PLoS One*, **8**, e77614.
15. Barria,C., Malecki,M. and Arraiano,C.M. (2013) Bacterial adaptation to cold. *Microbiology*, **159**, 2437–2443.
16. Alreshidi,M.M., Dunstan,R.H., Macdonald,M.M., Smith,N.D., Gottfries,J. and Roberts,T.K. (2015) Metabolomic and proteomic responses of *Staphylococcus aureus* to prolonged cold stress. *J. Proteomics*, **121**, 44–55.
17. Fang,L., Jiang,W., Bae,W. and Inouye,M. (1997) Promoter-independent cold-shock induction of *cspA* and its derepression at 37°C by mRNA stabilization. *Mol. Microbiol.*, **23**, 355–364.
18. Uppal,S., Akkipeddi,V.S.N.R. and Jawali,N. (2008) Posttranscriptional regulation of *cspE* in *Escherichia coli*: involvement of the short 5′-untranslated region. *FEMS Microbiol. Lett.*, **279**, 83–91.
19. Xia,B., Ke,H. and Inouye,M. (2001) Acquirement of cold sensitivity by quadruple deletion of the *cspA* family and its suppression by PNPase S1 domain in *Escherichia coli*. *Mol. Microbiol.*, **40**, 179–188.
20. Zhang,Y., Burkhardt,D.H., Rouskin,S., Li,G.-W., Weissman,J.S. and Gross,C.A. (2018) A stress response that monitors and regulates mRNA structure is central to cold shock adaptation. *Mol. Cell*, **70**, 274–286.
21. Schmid,B., Klumpp,J., Raimann,E., Loessner,M.J., Stephan,R. and Tasara,T. (2009) Role of cold shock proteins in growth of *Listeria monocytogenes* under cold and osmotic stress conditions. *Appl. Environ. Microbiol.*, **75**, 1621–1627.
22. Chapot-Chartier,M.P., Schouler,C., Lepeuple,A.S., Gripon,J.C. and Chopin,C. (1997) Characterization of *cspB*, a cold-shock-inducible gene from *Lactococcus lactis*, and evidence for a family of genes homologous to the *Escherichia coli cspA* major cold shock gene. *J. Bacteriol.*, **179**, 5589–5593.
23. Willimsky,G., Bang,H., Fischer,G. and Marahiel,M.A. (1992) Characterization of *cspB*, a *Bacillus subtilis* inducible cold shock gene affecting cell viability at low temperatures. *J. Bacteriol.*, **174**, 6326–6335.
24. Graumann,P., Wendrich,T.M., Weber,M.H., Schröder,K. and Marahiel,M.A. (1997) A family of cold shock proteins in *Bacillus subtilis* is essential for cellular growth and for efficient protein synthesis at optimal and low temperatures. *Mol. Microbiol.*, **25**, 741–756.
25. Duval,B.D., Mathew,A., Satola,S.W. and Shafer,W.M. (2010) Altered growth, pigmentation, and antimicrobial susceptibility properties of *Staphylococcus aureus* due to loss of the major cold shock gene *cspB*. *Antimicrob. Agents Chemother.*, **54**, 2283–2290.
26. Anderson,K.L., Roberts,C., Disz,T., Vonstein,V., Hwang,K., Overbeek,R., Olson,P.D., Projan,S.J. and Dunman,P.M. (2006) Characterization of the *Staphylococcus aureus* heat shock, cold shock, stringent, and SOS responses and their effects on log-phase mRNA turnover. *J. Bacteriol.*, **188**, 6739–6756.
27. Brandi,A. (1999) Massive presence of the *Escherichia coli* 'major cold-shock protein' CspA under non-stress conditions. *EMBO J.*, **18**, 1653–1659.
28. Giuliodori,A.M., Di Pietro,F., Marzi,S., Masquida,B., Wagner,R., Romby,P., Gualerzi,C.O. and Pon,C.L. (2010) The *cspA* mRNA is a thermosensor that modulates translation of the cold-shock protein CspA. *Mol. Cell*, **37**, 21–33.
29. Gualerzi,C.O., Maria Giuliodori,A. and Pon,C.L. (2003) Transcriptional and post-transcriptional control of cold-shock genes. *J. Mol. Biol.*, **331**, 527–539.
30. Goldstein,J., Pollitt,N.S. and Inouye,M. (1990) Major cold shock protein of *Escherichia coli*. *Proc. Natl Acad. Sci. U.S.A.*, **87**, 283–287.
31. Yamanaka,K., Mitta,M. and Inouye,M. (1999) Mutation analysis of the 5′ untranslated region of the cold shock *cspA* mRNA of *Escherichia coli*. *J. Bacteriol.*, **181**, 6284–6291.
32. Narberhaus,F., Waldminghaus,T. and Chowdhury,S. (2006) RNA thermometers. *FEMS Microbiol. Rev.*, **30**, 3–16.
33. Ignatov,D., Vaitkevicius,K., Durand,S., Cahoon,L., Sandberg,S.S., Liu,X., Kallipolitis,B.H., Rydén,P., Freitag,N., Condon,C. *et al.* (2020) An mRNA–mRNA interaction couples expression of a virulence factor and its chaperone in *Listeria monocytogenes*. *Cell Rep.*, **30**, 4027–4040.

34. Phadtare,S., Alsina,J. and Inouye,M. (1999) Cold-shock response and cold-shock proteins. *Curr. Opin. Microbiol.*, **2**, 175–180.
35. Wang,N., Yamanaka,K. and Inouye,M. (1999) CspI, the ninth member of the CspA family of *Escherichia coli*, is induced upon cold shock. *J. Bacteriol.*, **181**, 1603–1609.
36. Catalan-Moreno,A., Caballero,C.J., Irurzun,N., Cuesta,S., López Sagaseta,J. and Toledo-Arana,A. (2020) One evolutionarily selected amino acid variation is sufficient to provide functional specificity in the cold shock protein paralogs of *Staphylococcus aureus*. *Mol. Microbiol.*, **113**, 826–840.
37. Lioliou,E., Sharma,C.M., Caldelari,I., Helfer,A.C., Fechter,P., Vandenesch,F., Vogel,J. and Romby,P. (2012) Global regulatory functions of the *Staphylococcus aureus* endoribonuclease III in gene expression. *PLoS Genet.*, **8**, e1002782.
38. Zuker,M. (2003) Mfold web server for nucleic acid folding and hybridization prediction. *Nucleic Acids Res.*, **31**, 3406–3415.
39. Darty,K., Denise,A. and Ponty,Y. (2009) VARNA: interactive drawing and editing of the RNA secondary structure. *Bioinformatics*, **25**, 1974–1975.
40. Caballero,C.J., Menendez-Gil,P., Catalan-Moreno,A., Vergara-Irigaray,M., García,B., Segura,V., Irurzun,N., Villanueva,M., Ruiz de Los Mozos,I., Solano,C. *et al.* (2018) The regulon of the RNA chaperone CspA and its auto-regulation in *Staphylococcus aureus*. *Nucleic Acids Res.*, **46**, 1345–1361.
41. Lee,J.C. (1995) Electrotransformation of staphylococci. *Methods Mol. Biol.*, **47**, 209–216.
42. Balestrino,D., Hamon,M.A., Dortet,L., Nahori,M.-A., Pizarro-Cerda,J., Alignani,D., Dussurget,O., Cossart,P. and Toledo-Arana,A. (2010) Single-cell techniques using chromosomally tagged fluorescent bacteria to study *Listeria monocytogenes* infection processes. *Appl. Environ. Microbiol.*, **76**, 3625–3636.
43. Lee,G., Talkington,C. and Pero,J. (1980) Nucleotide sequence of a promoter recognized by *Bacillus subtilis* RNA polymerase. *Mol. Gen. Genet.*, **180**, 57–65.
44. Charpentier,E., Anton,A.I., Barry,P., Alfonso,B., Fang,Y. and Novick,R.P. (2004) Novel cassette-based shuttle vector system for Gram-positive bacteria. *Appl. Environ. Microbiol.*, **70**, 6076–6085.
45. Arnaud,M., Chastanet,A. and Debarbouille,M. (2004) New vector for efficient allelic replacement in naturally nontransformable, low-GC-content, Gram-positive bacteria. *Appl. Environ. Microbiol.*, **70**, 6887–6891.
46. Valle,J., Toledo-Arana,A., Berasain,C., Ghigo,J.-M., Amorena,B., Penadés,J.R. and Lasa,I. (2003) SarA and not sigma B is essential for biofilm development by *Staphylococcus aureus*. *Mol. Microbiol.*, **48**, 1075–1087.
47. Toledo-Arana,A., Dussurget,O., Nikitas,G., Sesto,N., Guet-Revillet,H., Balestrino,D., Loh,E., Gripenland,J., Tiensuu,T., Vaitkevicius,K. *et al.* (2009) The *Listeria* transcriptional landscape from saprophytism to virulence. *Nature*, **459**, 950–956.
48. Menendez-Gil,P., Caballero,C.J., Solano,C. and Toledo-Arana,A. (2020) Fluorescent molecular beacons mimicking RNA secondary structures to study RNA chaperone activity. *Methods Mol. Biol.*, **2106**, 41–58.
49. Krismer,B., Liebeke,M., Janek,D., Nega,M., Rautenberg,M., Hornig,G., Unger,C., Weidenmaier,C., Lalk,M. and Peschel,A. (2014) Nutrient limitation governs *Staphylococcus aureus* metabolism and niche adaptation in the human nose. *PLoS Pathog.*, **10**, e1003862.
50. Lasa,I., Toledo-Arana,A., Dobin,A., Villanueva,M., de los Mozos,I.R., Vergara-Irigaray,M., Segura,V., Fagegaltier,D., Penadés,J.R., Valle,J. *et al.* (2011) Genome-wide antisense transcription drives mRNA processing in bacteria. *Proc. Natl Acad. Sci. U.S.A.*, **108**, 20172–20177.
51. Lindemann,J., Leiacker,R., Rettinger,G. and Keck,T. (2002) Nasal mucosal temperature during respiration. *Clin. Otolaryngol. Allied Sci.*, **27**, 135–139.
52. Jiang,W., Hou,Y. and Inouye,M. (1997) CspA, the major cold-shock protein of *Escherichia coli*, is an RNA chaperone. *J. Biol. Chem.*, **272**, 196–202.
53. Phadtare,S. and Inouye,M. (1999) Sequence-selective interactions with RNA by CspB, CspC and CspE, members of the CspA family of *Escherichia coli*. *Mol. Microbiol.*, **33**, 1004–1014.
54. Sachs,R., Max,K.E.A., Heinemann,U. and Balbach,J. (2012) RNA single strands bind to a conserved surface of the major cold shock protein in crystals and solution. *RNA*, **18**, 65–76.
55. Shenhar,Y., Biran,D. and Ron,E.Z. (2012) Resistance to environmental stress requires the RNA chaperones CspC and CspE. *Environ. Microbiol. Rep.*, **4**, 532–539.
56. Michaux,C., Holmqvist,E., Vasicek,E., Sharan,M., Barquist,L., Westermann,A.J., Gunn,J.S. and Vogel,J. (2017) RNA target profiles direct the discovery of virulence functions for the cold-shock proteins CspC and CspE. *Proc. Natl Acad. Sci. U.S.A.*, **114**, 6824–6829.
57. Johansson,J., Mandin,P., Renzoni,A., Chiaruttini,C., Springer,M. and Cossart,P. (2002) An RNA thermosensor controls expression of virulence genes in *Listeria monocytogenes*. *Cell*, **110**, 551–561.
58. Waldminghaus,T., Heidrich,N., Brantl,S. and Narberhaus,F. (2007) FourU: a novel type of RNA thermometer in *Salmonella*. *Mol. Microbiol.*, **65**, 413–424.
59. Loh,E., Kugelberg,E., Tracy,A., Zhang,Q., Gollan,B., Ewles,H., Chalmers,R., Pelicic,V. and Tang,C.M. (2013) Temperature triggers immune evasion by *Neisseria meningitidis*. *Nature*, **502**, 237–240.
60. Weber,G.G., Kortmann,J., Narberhaus,F. and Klose,K.E. (2014) RNA thermometer controls temperature-dependent virulence factor expression in *Vibrio cholerae*. *Proc. Natl Acad. Sci. U.S.A.*, **111**, 14241–14246.
61. Righetti,F., Nuss,A.M., Twittenhoff,C., Beele,S., Urban,K., Will,S., Bernhart,S.H., Stadler,P.F., Dersch,P. and Narberhaus,F. (2016) Temperature-responsive *in vitro* RNA structurome of *Yersinia pseudotuberculosis*. *Proc. Natl Acad. Sci. U.S.A.*, **113**, 7237–7242.
62. Twittenhoff,C., Heroven,A.K., Mühlen,S., Dersch,P. and Narberhaus,F. (2020) An RNA thermometer dictates production of a secreted bacterial toxin. *PLoS Pathog.*, **16**, e1008184.
63. Loh,E., Righetti,F., Eichner,H., Twittenhoff,C. and Narberhaus,F. (2018) RNA thermometers in bacterial pathogens. *Microbiol. Spectrum*, **6**, RWR-0012-2017.
64. Altuvia,S., Kornitzer,D., Teff,D. and Oppenheim,A.B. (1989) Alternative mRNA structures of the cIII gene of bacteriophage lambda determine the rate of its translation initiation. *J. Mol. Biol.*, **210**, 265–280.
65. Hussein,H., Fris,M.E., Salem,A.H., Wiemels,R.E., Bastock,R.A., Righetti,F., Burke,C.A., Narberhaus,F., Carroll,R.K., Hassan,N.S. *et al.* (2019) An unconventional RNA-based thermosensor within the 5′UTR of *Staphylococcus aureus cidA*. *PLoS One*, **14**, e0214521.